frontiers | Frontiers in Ecology and Evolution

TYPE Original Research
PUBLISHED 17 March 2026
DOI 10.3389/fevo.2026.1351288

OPEN ACCESS

EDITED BY
Peter David Roopnarine,
California Academy of Sciences, United States

REVIEWED BY
Terry A. Gates,
North Carolina State University, United States
David Varricchio,
Montana State University, United States

*CORRESPONDENCE
Ming-Tsang Lee
mtlee@pme.nthu.edu.tw
Tzu-Ruei Yang
tzurueiyang@nmns.edu.tw

†PRESENT ADDRESS
Chun-Yu Su,
Department of Organismic and Evolutionary Biology, Harvard University, Cambridge, MA, United States
Jun-Yang Liao,
Thermal Design Department II, Inventec Corporation, Taipei, Taiwan

RECEIVED 06 December 2023
REVISED 18 January 2026
ACCEPTED 21 January 2026
PUBLISHED 17 March 2026

CITATION
Su C-Y, Liao J-Y, Wu H-J, Chou K-Y, Chen C, Lee M-T and Yang T-R (2026) Heat transfer in a realistic clutch reveals a lower efficiency in incubation of oviraptorid dinosaurs than of modern birds.
Front. Ecol. Evol. 14:1351288.
doi: 10.3389/fevo.2026.1351288

Heat transfer in a realistic clutch reveals a lower efficiency in incubation of oviraptorid dinosaurs than of modern birds

Chun-Yu Su[1†], Jun-Yang Liao[2†], Hsiao-Jou Wu[3], Kuan-Yu Chou[3], Ching Chen[3], Ming-Tsang Lee[2*] and Tzu-Ruei Yang[3,4,5*]

[1]Washington High School, Taichung, Taiwan, [2]Department of Power Mechanical Engineering, National Tsing Hua University, Hsinchu, Taiwan, [3]Department of Geology, National Museum of Natural Sciences, Taichung, Taiwan, [4]Department of Earth Sciences, National Cheng Kung University, Tainan, Taiwan, [5]Department of Life Sciences, National Chung Hsing University, Taichung, Taiwan

It has been proposed that some reproductive traits specific to birds, such as thermoregulatory contact incubation (TCI), may also have been present in oviraptorosaurians, as inferred from clutch-associated oviraptorid adults with postures resembling avian brooding behavior. Nevertheless, prerequisites for TCI, such as the incubating adult providing the majority of heat needed for normal embryonic development, have not been evaluated with respect to their body and egg dimensions. To test this, a realistic *Heyuannia huangi* incubator, oviraptorid clutches, and heat transfer numerical simulations were developed to simulate the brooding behavior of *Heyuannia huangi* and *Nemegtomaia barsboldi*. Our results indicate that the incubator could only partially contact the outer-ring eggs of the clutch, leading to a temperature difference between the inner and outer rings and a lower incubation efficiency compared to that of extant birds. Additionally, an outer-ring egg had a considerably higher temperature than the superimposed inner-ring egg when positioned near the incubator's core, whereas an outer-ring egg had approximately the same temperature as the superimposed inner-ring egg when positioned closer to the incubator's periphery. If *Nemegtomaia barsboldi* were to initiate incubation before clutch completion, the temperature distribution could cause the outer-ring egg at the incubator's core to hatch earlier than the inner-ring egg immediately beneath it, whereas at the periphery the inner-ring egg could hatch earlier than the outer-ring egg immediately above it. However, irrespective of position, the inner-ring egg of *Heyuannia huangi* may hatch earlier than the outer-ring egg immediately above it. Our findings do not support the TCI hypothesis and instead, they suggest that oviraptorids co-regulated incubation with environmental heat, with the adult stabilizing clutch temperatures, reducing thermal extremes, and influencing patterns of asynchronous hatching.

KEYWORDS

asynchronous hatching, heat transfer, *Heyuannia huangi*, *Nemegtomaia barsboldi*, numerical simulation, oviraptorosaurians, reproductive biology, thermoregulatory contact incubation

1 Introduction

Paleontologists frequently infer dinosaur behaviors by phylogenetically bracketing the two closest extant relatives of dinosaurs, crocodiles and birds (Neornithes) (Sato et al., 2005; Organ et al., 2007; Tanaka et al., 2018a; Chapelle et al., 2020). In terms of reproductive behavior facilitating egg development, however, crocodiles and birds differ to a great extent. Crocodiles bury their eggs in substrates and rely on environmental heat sources, such as sunlight or fermentation of nest substrates (Deeming, 2006; Tanaka et al., 2015). Conversely, all bird eggs, excluding megapode and some Charadriiformes eggs (Dekker, 2007), are exposed to the air. Some of them are manipulated during incubation to receive heat from the featherless brooding patch of the incubating adult, a behavior known as effective incubation (Wang and Beissinger, 2011), contact incubation (Deeming, 2002; Turner, 2002), or thermoregulatory contact incubation (TCI) (Yang et al., 2019a, 2019b). Based on extant bird species, TCI is defined as: (i) all eggs are contacted by the incubating adult (Deeming, 2002; Wang and Beissinger, 2011); (ii) the incubating adult is the major heat source that keeps the embryos at temperature suitable for development (Deeming, 2002); (iii) the temperature differences between the eggs are small, resulting in similar embryonic developmental rates (Deeming, 2002; Yang et al., 2019a, 2019b). While most pre-Pennaraptora dinosaurs, with the exception of Argentinian Auca Mahuevo sauropods (Chiappe et al., 2004; Jackson et al., 2008), could have buried their eggs, some, such as oviraptorosaurians and troodontids, built semi-open nests (Varricchio et al., 1997, 1999, 2013; Tanaka et al., 2015, 2018b; Wiemann et al., 2017). Given the intermediate characteristics of these semi-open nests, it remains unclear whether the adults incubated the nests as modern birds do or relied on environmental heat sources as crocodiles do.

The adult-associated clutches of oviraptorid dinosaurs found in Cretaceous strata in China and Mongolia could elucidate the origin of TCI (Osborn et al., 1924; Dong and Currie, 1996; Clark et al., 1999; Fanti et al., 2012; Norell et al., 1995, 2018; Bi et al., 2021). So far, seven oviraptorid specimens have been found in association with clutches, each sitting on top of an oviraptorid clutch and exhibiting a bird-like brooding posture: forelimbs spreading across the rim of the clutch, folded hindlimbs resting on the eggs, and belly contacting the egg-free center of the clutch (Osborn et al., 1924; Dong and Currie, 1996; Clark et al., 1999; Fanti et al., 2012; Norell et al., 1995, 2018; Bi et al., 2021). In these specimens, a thin layer of sediment lies between the adult and the eggs, and, in some cases, the adult is in "extremely close proximity" to the eggs (Bi et al., 2021). Some paleontologists interpret the adult-associated clutches as demonstrations of TCI behavior (Dong and Currie, 1996; Clark et al., 1999; Fanti et al., 2012; Norell et al., 1995, 2018; Bi et al., 2021), a hypothesis that is supported by the discovery of embryonic remains in *Macroolithus yaotunensis* eggs covered by an oviraptorid skeleton from the Nanxiong Group in southern China (Bi et al., 2021). A study of eggshell porosity also reveals that oviraptorids are the phylogenetically earliest dinosaur group known to build semi-open nests and exercise some avian-like reproductive features and behaviors (Tanaka et al., 2015). For instance, oviraptorid eggshells have cuticles and blue-green pigmentation, which are associated with paternal care (Wiemann et al., 2017, 2018; Yang et al., 2018). Their embryos may hatch asynchronously, as in some derived Neoaves (Weishampel et al., 2008; Yang et al., 2019a; Bi et al., 2021), and exhibit prehatching postures resembling avian tucking behavior (Xing et al., 2021).

Despite the similarities between oviraptorid and avian reproductive traits, oviraptorid clutches, *sensu* Yang et al. (2019b), are unanalogous among extant species. In contrast to the *en masse* style of egg laying seen in crocodiles and some sauropods (Seymour, 1979; Grellet-Tinner and Fiorelli, 2010; Reisz et al., 2012; Ruxton et al., 2014), oviraptorid eggs are arranged in pairs, a feature that has been linked to the two functional oviducts ovulating monoautochronically (Varricchio et al., 1997; Sato et al., 2005; Jin et al., 2019). Some egg pairs have different maternal origins, as supported by the differences in phosphorus distribution patterns and shell thicknesses between egg pairs, suggesting communal nesting behavior (Yang et al., 2016; Weiß, 2020). These egg pairs have their acute end buried and blunt end exposed in the air (Wiemann et al., 2017). They form rings encircling the central vacant space, with the blunt ends pointing towards the center in a 35° to 40° inclination angle relative to the ground (Yang et al., 2019b). In clutches with multiple rings of eggs, the outer ring stacks on top of the inner ring to form tiers, and a thin layer of sediment is interbedded between the rings (Yang et al., 2019b). The highly organized structure suggests that oviraptorosaurians laid eggs sequentially from the innermost ring to the outermost ring (Yang et al., 2019b).

Based on the unique clutch structure and the inferred clutch-building behavior, some researchers have questioned the validity of directly inferring TCI behavior based on the adult-associated clutch specimens (Deeming, 2002; Yang et al., 2019b). The stacked structure of the clutch suggests that the outer ring may have prevented the adult from contacting the inner-ring eggs; whereas the egg-free center may lead to insufficient contact between the adult and the eggs as the adult's belly would have rested primarily over the egg-free center (Deeming, 2002; Yang et al., 2019b). Furthermore, inferring from the highly organized and minimally disturbed clutch architecture, oviraptorid eggs are hypothesized to have no chalazae (Varricchio et al., 1997), further preventing the parents from manipulating them to distribute heat evenly (Yang et al., 2019b, *contra* Yang and Sander, 2022). Despite these speculations against oviraptorids utilizing TCI, the TCI prerequisite of the adult sufficiently contacting every egg has not been tested.

Regarding the TCI prerequisite of the incubating adult being the primary heat source elevating the clutch over ambient conditions, several isotopic studies indicate that oviraptorids had body and incubation temperatures similar to those of birds. Analyses of

Abbreviations: HYMV, Heyuan Museum, Guangdong Province, China; IGM, Mongolian Institute for Geology, Ulaanbaatar, Mongolia; LDNH, Lande Museum of Natural History, Hebei Province, China; NMNS, National Museum of Natural Sciences, Taichung City, Taiwan.

oviraptorid eggshells from the Nemegt and Djadokhta formations reveal that the adult had a body temperature of 31.9 ± 2.9°C (Eagle et al., 2015), and the embryos from the Nanxiong Group were incubated at temperatures ranging from 30°C to 40°C (Amiot et al., 2017; Bi et al., 2021). Despite our poor understanding of the optimal incubation temperature for oviraptorid embryos, the presence of late-stage embryos at the aforementioned temperature range suggests that the isotopic temperature estimates could be the developmental temperature range of oviraptorid embryos. However, the ambient temperature, 34°C on average, of the Late Cretaceous Nanxiong Group could exceed these incubation temperature ranges (Ma et al., 2018), and it remains unclear whether the eggs mainly received heat from the adult or the environment (Deeming, 2002). Even though the egg temperature might be maintained at a viable range regardless of the main heat source, there might exist temperature differences between the eggs.

For the third prerequisite, the adult's ability to maintain all eggs within a constrained temperature range is challenged by the discovery of embryos exhibiting different levels of ossification (Weishampel et al., 2008; Yang et al., 2019a; Bi et al., 2021). In extant saurians, the rate of embryonic development correlates positively with the incubation temperature, up to the lethal threshold (Hutton, 1987; Deeming and Ferguson, 1991; Lang and Andrews, 1994; Hepp et al., 2006; Parker and Andrews, 2007; Zhao et al., 2015). Since avian eggs are incubated within a narrow thermal range, asynchronous hatching, defined as a spread of hatching greater than 24 hours (Stoleson and Beissinger, 1995), usually results from the adult commencing TCI prior to clutch completion (Stoleson and Beissinger, 1995; Wang and Beissinger, 2011; *contra* Griffith et al., 2016). To date, three partially preserved oviraptorid clutches bearing embryos with different levels of ossification have been discovered in the Nanxiong Group (Weishampel et al., 2008; Yang et al., 2019a; Bi et al., 2021). Two of the three partial clutches have distinguishable inner and outer rings. Of these, Yang et al. (2019a) describe a partial clutch containing a pair of inner-ring embryos and a single outer-ring embryo. To explain a higher level of ossification in the inner-ring embryos than the outer-ring one, Yang et al. (2019a) propose two possible scenarios. The first one is that oviraptorids practiced "effective" TCI before clutch completion as some birds do (Yang et al., 2019a). The second is that oviraptorids initiated incubation after clutch completion but did not utilize effective TCI or incubate at all, such that the developmental levels of the eggs reflect the order in which they were laid (Yang et al., 2019a). In contrast, Bi et al. (2021) describe another clutch in which an inner-ring egg exhibits a lower developmental level than an outer-ring egg in an adult-associated, embryo-bearing clutch, contradicting the pattern reported by Yang et al. (2019a). The authors postulate that the adult came to "brood" after clutch completion and the outer ring developed faster due to closer contact with the adult and correspondingly higher incubation temperature (Bi et al., 2021). Further isotopic analyses reveal intra-ring temperature variation in the outermost ring, though the inter-ring temperature variation remains unknown (Bi et al., 2021). While both studies consider temperature difference as the major attribute of inter-ring asynchronous hatching, support of such inferences still requires further investigations of temperature distribution within the clutch.

In addition to estimating temperatures of extinct species based on stable oxygen isotope composition ($\delta^{18}O$) and clumped isotope paleothermometry (Δ^{47}) (Eagle et al., 2015; Amiot et al., 2017; Bi et al., 2021), some studies have conducted heat transfer experiments or numerical simulations to study dinosaur physiology (Farlow et al., 1976; O'Connor and Dodson, 1999; Bourke, 2015; Hartman et al., 2022). While these realistic or *in silico* studies make generalizations based on extant proxies, they yield illuminating insights into dinosaur physiology and behaviors. Regarding dinosaur brooding behaviors, Hogan and Varricchio (2021) simulated troodontid incubation by heating two half-buried chicken eggs with a water bag and concluded that buried dinosaur eggs like those of troodontids could have been maintained above ambient temperature via adult-mediated incubation. Although the authors inferred from the experimental results that the inner ring of an oviraptorid clutch would have experienced a lower temperature than the outer ring due to the thermal gradient, the oversimplified model was likely insufficient to explain the heat transfer in a much more complex oviraptorid clutch. Taking a similar approach, Hogan (2024) reconstructed a generalized oviraptorid clutch using emu eggs and tested the thermal effects of oviraptorid incubation under the scenarios of the incubator directly contacting the eggs from the top, indirectly through sandy substrates, and directly contacting with additional heat source within the clutch that simulates the hindlimbs of the adult. Based on the results, the author proposes that oviraptorids could achieve more uniform temperatures between rings when hindlimbs are present within the clutch and the brooding behavior could confer thermal advantage favoring subaerial clutch arrangement. While Hogan (2024) makes an important leap in experimentally testing the thermal effects of incubating an oviraptorid clutch, there are a few less realistic reconstructions. The radially symmetrical design of the incubator is drastically different from the bilaterally symmetric, elongated body of an oviraptorid adult. Additionally, the much higher breadth-to-length ratio of emu eggs than oviraptorid eggs leads to a more packed clutch and more exposed eggs than those observed in fossil records. Regarding the experimental setting, conducting the experiments indoors overlooks the contribution of ambient heat sources and the diel fluctuation of ambient temperatures. An even more realistic reconstruction is needed to properly assess the thermal effects of incubation on an oviraptorid clutch.

Taking into account the effects of adult body dimensions, elongated egg shapes, clutch arrangement, and environmental heat sources, this study investigates the brooding behavior and asynchronous hatching patterns of oviraptorid dinosaurs through realistic heat transfer experiments and *in silico* numerical simulations. These pioneering approaches will not only contribute to the discussion on the early evolution of TCI behavior but also illuminate the unique mechanisms underlying asynchronous hatching in oviraptorid dinosaurs.

2 Materials and methods

2.1 Incubation experiments

To study the thermodynamic effects of an oviraptorid adult attending a clutch, a life-sized oviraptorid incubator, oviraptorid eggs, and clutches were reconstructed. Each component is introduced as follows.

2.1.1 Oviraptorid incubator

A life-sized *Heyuannia huangi* body model was constructed using polystyrene foam and wood for the skeletal framework, and cotton, bubble paper, and cloth for soft tissue. *Heyuannia huangi* was chosen as the model because both it and its egg *Macroolithus yaotunensis* have been well studied (Lü, 2003; Cheng et al., 2008; Sato et al., 2005; Wiemann et al., 2017, 2018; Yang et al., 2018, 2019a; Bi et al., 2021). In the oviraptorid adult-associated clutches (Osborn et al., 1924; Dong and Currie, 1996; Clark et al., 1999; Fanti et al., 2012; Norell et al., 2018; Bi et al., 2021), the clutch was primarily covered by the trunk region (limbs included) from the first dorsal vertebra to the posterior tip of the ilium (Clark et al., 1999; Norell et al., 2018; Bi et al., 2021). Accordingly, the head, neck, and tail were not reconstructed in the model.

The lengths of long bones (femur and tibia) of *Heyuannia huangi* were acquired from specimens HYMV1–1 and HYMV1–2 in Lü (2003). Since the width and the height of the *Heyuannia huangi* holotype were not available due to poor preservation, the width was approximated with an oviraptorid *Nemegtomaia barsboldi* skeleton displayed at the National Museum of Natural Science, Taiwan (NMNS) based on the reason that *Nemegtomaia barsboldi* is the sister taxon of *Heyuannia* with a similar body length (Fanti et al., 2012; Funston, 2020). Transverse planes were constructed at an interval of 7.5 cm (2.5% of the total body length of the *Nemegtomaia barsboldi* skeleton; Seebacher, 2001) starting from the first dorsal vertebra to the posterior tip of the ilium. In each transverse plane, the width (twice the maximum medial-lateral distance of the right rib cage) was measured. Given that the body size (mass) is positively correlated with the length of the long bones (Christiansen, 1999a, 1999b; Campione and Evans, 2012), the measured widths were rescaled using the average of the femoral length ratio between *Heyuannia huangi* and *Nemegtomaia barsboldi* and the tibial length ratio between the two species, a value of 0.947, to estimate the width of *Heyuannia huangi* in each transverse plane.

Since the NMNS *Nemegtomaia barsboldi* skeleton lacked gastralia, the height (the dorsal-ventral distance from the tip of the spinous process, or the linearly interpolated height between the two neighboring spinous process, to the gastralia) of each transverse plane was estimated with the *Heyuannia huangi* reconstruction illustrated by Scott Hartman (Hartman, 2003). Height measurements were taken at an interval of 7.1 cm (7.5 cm × 0.947). The dorsal-ventral distance from the tip of the spinous process to the width of the right rib cage of each transverse plane of the *Nemegtomaia* skeleton was also measured and rescaled (× 0.947) to calculate the intersection point between the width and the height in the *Heyuannia* model (Figure 1). These transverse planes were then lofted to create the trunk region.

The internal structure in the *Heyuannia* model was supported by polystyrene foam with a cross-section of 4 cm × 5.4 cm. Wood with a cross-section of 0.9 cm × 0.9 cm was cut into the dimensions of calculated widths and heights. The wood pieces were inserted into the foam every 7.1 cm and intersected perpendicularly at the intersection point of each transverse plane. After gluing the cross-like structure along the foam, cotton and bubble wrap were packed into the remaining space to represent flesh. A piece of blue cloth covered the exterior of the model. The final model measured 63.9 cm in length, 45.6 cm at its widest point, and 33.2 cm at its deepest section (Figure 1).

After the *Heyuannia* model was completed, a heating pad (THOMSON Electric Blanket SW-W03BS) was attached to the ventral side of the model as the heat source. The body model and the heating pad together constituted the oviraptorid incubator. The portion of the pad that encircled the model represented the belly of the brooding oviraptorid, hereinafter referred to as the "core". The folded-up portion of the heating pad resembled the limbs of an adult covering the rim of the clutch, hereinafter referred to as the "periphery" (Figure 2). Although feathers had so far been found in basal oviraptorosaurians, many studies suggested that feathers were a shared characteristic in Oviraptorosauria (Hopp and Orsen, 2004; Foth et al., 2014; Ksepka, 2020). A piece of approximately 0.3 cm-thick blanket (synthetic fiber and polar fleece) covered the incubator to mimic the insulative effect of feathers (Figure 2). The incubator was positioned on the clutch based on the postures of IGM100/979, IGM100/1004, and LDNHMF2008, with the anterior end (first dorsal vertebra), the posterior end (posterior tip of the ilium), and the limbs (represented by the folded heating pad) contacting the rim of the clutch (Clark et al., 1999; Norell et al., 2018; Bi et al., 2021).

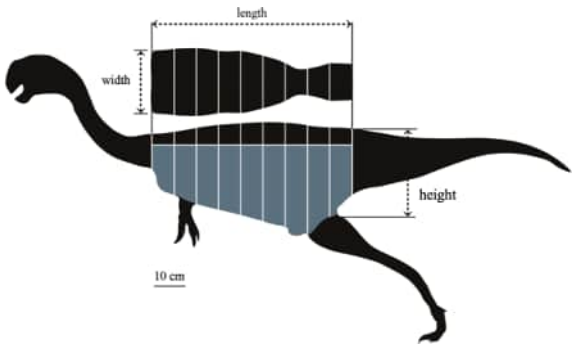

FIGURE 1
Dorsal and lateral views of the *Heyuannia* model. Width and height measurements were taken at each transverse plane (the white vertical line) starting from the first dorsal vertebra to the posterior tip of the ilium (model length). The distance from the tip of the spinous process to the width of the rib cage of each transverse plane was subtracted from the height when constructing the model, as indicated by the blue region in the lateral view. The *Heyuannia* silhouette was adapted from Hartman (2003).

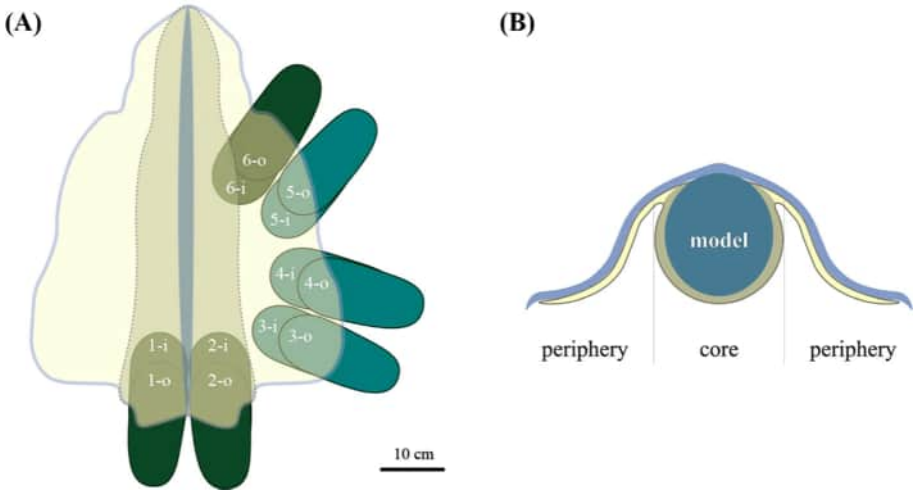

FIGURE 2
The core and the periphery of the incubator. **(A)** The dorsal view of the incubator lying on top of the eggs. The egg sets that contact the brown-yellow core with a dashed line [axis region of the adult body, see core in **(B)**] are core sets and have a dark-green color. The egg sets that contact the light-yellow periphery [appendicular region of the adult body, see periphery in **(B)**] are peripheral sets and have a blue-green color. The blanket [light-blue cover in **(B)**] is indicated by the outermost light-blue line of the incubator. **(B)** The transverse section of the incubator. The yellow heating pad is attached to the ventral side of the *Heyuannia* model. The brown-yellow portion of the heating pad that covers the model is the core, while the light-yellow portion that does not cover the model is the periphery. The light-blue blanket covers the model and the heating pad from the dorsal side.

2.1.2 Eggs

Modeling clay was molded into an oviraptorid egg shape based on the dimensions of NMNS CYN-2004-DINO-05, which had been previously assigned to *Macroolithus yaotunensis* (Wiemann et al., 2017). The blunt end of the clay egg was attached to a clay egg cup. About 60 g of casting resin was applied on the surface of the clay egg and a layer of fiberglass was attached to the resin to reinforce the shell. After the resin hardened, about 50 g of resin was evenly spread on the first resin layer. The resin egg was then detached from the clay egg cup and heated at 60 °C to melt the modeling clay from the blunt-end opening, leaving a hollow resin egg with a shell thickness ranging from 1.6 to 1.9 mm, a value consistent with the thickness of the *Macroolithus* eggshell (Yang et al., 2019b; Weiß, 2020). Lids (blunt ends) were made following the same procedure and attached to the resin eggs.

Inside each hollow resin egg, water was chosen to represent egg white based on their similar heat transfer performances (Sabliov et al., 2002). To measure the temperature of the blunt end, where the adult's belly would have contacted, and the embryo would have occupied (Turner, 2002; Yang et al., 2019a), a hole was drilled to insert a thermometer [digital thermometer NTC (10K/3435)] 2.5 cm into the water-filled cavity. After the hole was sealed with resin, waterproof paint (Aqua Seal: Mold and Mildew Resistant) was applied to the egg to reduce water loss.

The eggs' lengths (the distance between the tips of the blunt end and the acute end) ranged from 19.3 cm to 21.2 cm, and the widest widths ranged from 7.3 cm to 8.3 cm. The eggs weighed between 740 g and 867 g, falling within the estimated weight range of *Macroolithus* eggs (Tanaka et al., 2018a). The overall dimensions of the eggs were similar to those described in Bi et al. (2021). These eggs were repeatedly used throughout the experiments. Due to water loss, some eggs were repaired by injecting water into the eggs with needles until the eggs reached their original weights.

2.1.3 Clutches

Two types of clutches were reconstructed using the abovementioned resin *Macroolithus* eggs, an original clutch and a generalized clutch. The original clutch replicated the egg arrangement of the double-ring clutch NMNS004529-F003855 (see Yang, 2012). The eggs in this clutch had linearituberculate ornamentation, which only appeared in *Macroolithus* sp. among all *Elongatoolithidae* eggs (Zhao, 1975; Yang et al., 2019b; Weiß, 2020). Based on the ornamentation, the lengths, and the widest width of the eggs, the eggs were assigned to *Macroolithus*. After measuring the eggs' squashed inclination angles relative to the ground, the reconstructed angles were calculated based on the formula in Yang et al. (2019b). To avoid inaccurate estimation caused by deformation during fossilization, only eggs with intact blunt ends were included, yielding an average inclination angle of 29.6°, a value less than that reported in Yang et al. (2019b). There were 19 eggs in the specimen, but either because of deformation or burial by sediment, only 13 eggs could be reconstructed. The outer-ring eggs were labeled from 1 to 9. The inner-ring eggs were labeled from 10 to 13 and were located below egg 1, 2, and 3 (see Supplementary Figure S1). The eggs were positioned according to the observed arrangement in the clutch. For the eggs excluded in the reconstruction, the clutch rim was built to the height of the neighboring outer-ring eggs. The blunt ends pointed towards the clutch center at the reconstructed angles, and approximately five centimeters from the tip of the blunt end was exposed in the air (Wiemann et al., 2017). A one-centimeter-thick layer of soil laid between the two rings of the clutch. The soil thickness covering the

outermost ring was unknown but assumed to be one centimeter thick (Yang et al., 2019b). While the original clutch was more realistic than the generalized clutch, the small number of inner-ring eggs makes a comparison of the incubation effects on the inner- and outer-ring eggs difficult. To better compare the temperatures of the inner-ring eggs and the superimposing outer-ring eggs, a generalized clutch with parameters like that of the original clutch was constructed.

The generalized clutch had a configuration following several published complete clutches (Wiemann et al., 2017; Tanaka et al., 2018a; Yang et al., 2019b). In these fossils, the egg-free center was oval; the central angle between the egg pairs varied; the outer ring did not stack precisely on top of the inner ring; and each egg had a different inclination angle (Wiemann et al., 2017; Tanaka et al., 2018a; Yang et al., 2019b). Nevertheless, in the generalized clutch, the center was assumed to be a circle with a diameter of 24 cm; the outer ring stacked directly on top of the inner ring; and the eggs uniformly had 30° inclination relative to the ground. A one-centimeter-thick soil layer was laid between the two rings. As a complete clutch, it would have been a double-ring clutch with each ring consisting of 5 pairs, with a central angle of 20° within the egg pairs and 50° between the egg pairs. To simplify the experiment, only three out of the five pairs were reconstructed for the experiments. There were twelve eggs in total in the generalized clutch, with six in the inner ring and six in the outer ring. The eggs in the outer ring were named from 1-o to 6-o ("o" denotes outer). The inner-ring eggs were named from 1-i to 6-i ("i" denotes inner) (Figure 2A). Each stacked pair of inner- and outer-ring eggs was collectively referred to as a set (e.g., set 1 consists of egg 1-o and egg 1-i). There were two eggs per set, six sets in total. Egg 1-o, 2-o, and 6-o were contacted by the core of the incubator (hereinafter referred to as the "core eggs"). Other eggs were contacted by the periphery of the incubator (hereinafter referred to as the "peripheral eggs") (Figure 2).

As oviraptorid *Elongatoolithidae* eggs had been discovered in fine-grained (in China) and coarse-grained (in Mongolia) soil, soil composition of the clutch substrate might be less important to oviraptorids than to other buried nesters, which had specific preferences for soil for incubation (Tanaka et al., 2018b). Even so, we collected soil from the experimental site (24°04'15.4"N 120° 45'18.1"E) as it texturally resembled the sandy paleosol in the Nanxiong Group and Nemegt Formation (Fanti et al., 2012; Ma et al., 2018; Bi et al., 2021). When dried, it had a bulk density (1460 kg/m^3) similar to that of sandy loam (Robin et al., 1997). Since the composition, moisture, porosity, and bulk density of the soil can influence its thermal conductivity (Yang et al., 2005), experimenting with a similar type of soil better approximated heat transfer of the adult-associated clutch.

2.1.4 Experiments

Three experiments were performed to study the thermodynamic effects of clutch attendance: the absence of an adult (Experiment I), clutch attendance in a colder environment that resembled the temperature of the Nemegt Formation (Experiment II), and clutch attendance in a hotter environment that resembled the temperature of Nanxiong Group (Experiment III). All experiments were performed outdoors on a hill in Wufeng District, Taichung City, Taiwan (24° 04'15.4"N 120°45'18.1"E). Thermometers (digital thermometer NTC (10K/3435)) were calibrated in air, water, and local soil before the experiment and all measured within 0.3 °C of the mean. Temperatures were recorded manually every twenty minutes and compiled in Excel. Soil moisture (volumetric water content) of the clutch was measured at two locations at the start and the end of each experiment using two Capacitive Moisture Sensors v1.2 powered by an Arduino Uno board. These sensors were calibrated beforehand using local soil with different moisture levels. The correlation coefficient between the measured and observed moisture level was 0.94.

2.1.4.1 Experiment I: no incubator

This scenario was designed to simulate an oviraptorid clutch incubated by the environmental heat sources. In Experiment I, the original clutch was exposed directly to the sun without the incubator. It started at 7:06 and ended at 18:06 on October 17, 2021, totaling eleven hours. The weather was sunny with few clouds. A total of 29 thermometers was used: 13 measured the temperatures of the eggs' blunt ends, 2 measured the ambient (shaded air) temperature, and the rest measured the temperature of the soil between the eggs of the same pair at a depth equivalent to that of the base of the clutch (0 cm above the ground), the inner ring (12 cm above the ground), and the outer ring (18 cm above the ground).

2.1.4.2 Experiment II: incubator in a cold environment

Experiment II simulated the incubation of *Nemegtomaia barsboldi* in the Nemegt Formation based on the similarity in body size between *Heyuannia huangi* and *Nemegtomaia barsboldi*. It was performed from 8:03 to 23:03 on December 19, 2021. In Experiment II, the generalized clutch was incubated by the incubator, which was assumed to be a steady incubator without on- or off-bout behaviors (Turner, 2002). According to the meteorological station G2F820 of the Central Weather Bureau in Wufeng, Taichung (agr.cwb.gov.tw/NAGR/history/station_hour), the average ambient temperature of December 19 was 18.9 °C, which resembled that of the continental "cool temperate monsoon-influenced climate" of the Nemegt Formation (Owocki et al., 2020). Although the egg length of *Nemegtomaia barsboldi* was slightly shorter than that of *Heyuannia huangi*, *Nemegtomaia barsboldi* had a larger clutch-body ratio and thus was apparently unable to cover every egg (Fanti et al., 2012; Yang et al., 2019b). As less-covered eggs were prone to having a lower temperature (Boulton and Cassey, 2012), *Nemegtomaia barsboldi* eggs might have been incubated at a similar or lower temperature than that documented in Experiment II. However, it should be noted that the *N. barsboldi* associated clutch specimen (MPC-D 107/15) showed much poorer preservation than the other oviraptorid-associated clutch specimens, e.g., *Khaan* or *Citipati*, and thus the coverage of the eggs in the *N. barsboldi*-associated clutch specimen might have been underestimated (Fanti et al., 2012; Hogan, 2024).

Before Experiment II began, the eggs had been left undisturbed in the clutch for a night to reach thermal equilibrium with the

surrounding soil. When the experiment began, the cranial end of the incubator pointed towards egg 1-o and egg 2-o, and the caudal end pointed towards egg 6-o. The blanket, mimicking feathers, covered the incubator and contacted the clutch rim at about 15 cm above the ground. Most theropods were endothermic (Amiot et al., 2006), and birds fluffed up their feathers when the ambient temperature dropped (Veghte and Herreid, 1965). To maintain the body temperature of the incubator, an extra layer of blanket was added when the ambient temperature was at 22°C. Another piece of blanket was added at 18°C, but it did not cover the periphery of the incubator. A total of 31 thermometers were used: 12 measured the temperatures of the eggs' blunt ends, 2 measured the ambient (unshaded air) temperature, 3 measured the incubator's core and periphery temperature, 9 measured the temperature of the soil between the eggs of the same pair at various depths of the soil (same as Experiment I), and 3 measured the soil temperature in close proximity to the incubator at various depths of the soil (same as Experiment I). In the air gap, which was the space between the incubator and the interior clutch wall, a thermometer was placed at the center right above the soil and another was hung down about two centimeters from the incubator belly to measure the temperature gradation (Figure 3).

2.1.4.3 Experiment III: incubator in a hot environment

Experiment III simulated the clutch attendance of *Heyuannia huangi* in the Nanxiong Group. It was performed from 07:13 on July 25 to 13:13 on July 26, 2022. According to the meteorological station G2F820, the average air temperature on July 25 was 30.2°C, which was approximately 4°C lower than the upper end of the reconstructed paleotemperature range in the Nanxiong Group (Ma et al., 2018). Since the maximum temperatures of the eggs were highly influenced by the ambient temperature, it was possible that, back in the Cretaceous, *Heyuannia huangi* eggs might have experienced an incubation temperature equal to or higher than that documented in this experiment.

The generalized clutch was rebuilt using nine of the renewed eggs and three new eggs. A partial clutch for reference, which consisted of one outer-ring egg stacked on top of two inner-ring eggs, was placed nearby and exposed to the sun to serve as a control for the effect of incubation. The incubator was positioned on the generalized clutch as in Experiment II, while the referencing partial clutch was not incubated. A total of 80 thermometers were used to better document the environmental conditions for heat transfer simulation. In addition to what was recorded in Experiment II, more thermometers were placed on the soil surface (height relative to the ground same as Experiment I) to record the surface soil temperature. Air temperature measurers made from chopsticks and rubber bands measured the air temperature in close proximity to the surface thermometers (Figure 3). One additional thermometer measured the middle of the periphery of the incubator. Temperature data at 02:13, 02:53, and 03:13 were not collected. At 05:28, July 26, a tent temporarily covered the clutch to protect the thermometers from getting wet in the rain, and it was removed after the rain stopped at 05:44. During this period, the sky remained fully cloudy.

2.1.5 The contact area between the eggs and the incubator

After Experiments II and III, the exposed surfaces of the eggs were colored by acrylic paint. The incubator, with a piece of white cloth fastened on its ventral side, was then placed on top of the clutch in the same posture as during the experiments. The colored spot on the cloth was later analyzed with ImageJ (https://imagej.nih.gov/ij/) to represent the contact areas between the incubator and the eggs.

2.1.6 Data processing

Arithmetic means of incubation temperatures were calculated for comparison of temperature distribution between inner- and outer-ring eggs. The egg temperatures of the final four hours of Experiment II were averaged arithmetically. For Experiment III that had fluctuating egg temperature, the readings over a 24-hour period were arithmetically averaged based on the linear degree-hours model (Georges et al., 1994).

Furthermore, for egg temperatures that reached equilibrium, the adult incubation efficiency was calculated using Equation 1, which was modified from Hogan and Varricchio (2021), to assess the incubator's efficiency in elevating the egg's temperature above the ambient temperature.

$$\frac{the\ \ average\ \ egg\ \ temperature - the\ \ average\ \ ambient\ \ temperature}{the\ \ average\ \ incubator\ \ temperature - the\ \ average\ \ ambient\ \ temperature} \times 100\,\% \quad (1)$$

The original equation in Hogan and Varricchio (2021) used the difference between the maximum incubator temperature and the lowest ambient temperature in the denominator. The modified efficiency equation better accounts for the average contribution of the incubator's temperature to the egg's temperature, while preventing an arbitrarily low ground temperature value from influencing the calculation of the difference, as intended in Hogan and Varricchio (2021). The substitution of extremum values with average values in the equation is especially important in experimental settings with fluctuating ambient temperatures.

Among the experiments, only the eggs in Experiment II reached equilibria. While some of those eggs only reached equilibria in the final four hours, estimating the incubation efficiency solely from the final four hours would provide an overestimation since the contribution of environmental heat to egg temperatures is discounted by the declining ambient temperature after sunset. To avoid overestimation of the incubation efficiency, temperature data from the final seven hours of the experiment were used to calculate the incubation efficiency.

2.2 Heat transfer numerical simulation

2.2.1 The design of studies and boundary conditions

Two types of heat transfer numerical simulations were designed —the posture simulations and the non-posture simulations—and

10.3389/fevo.2026.1351288

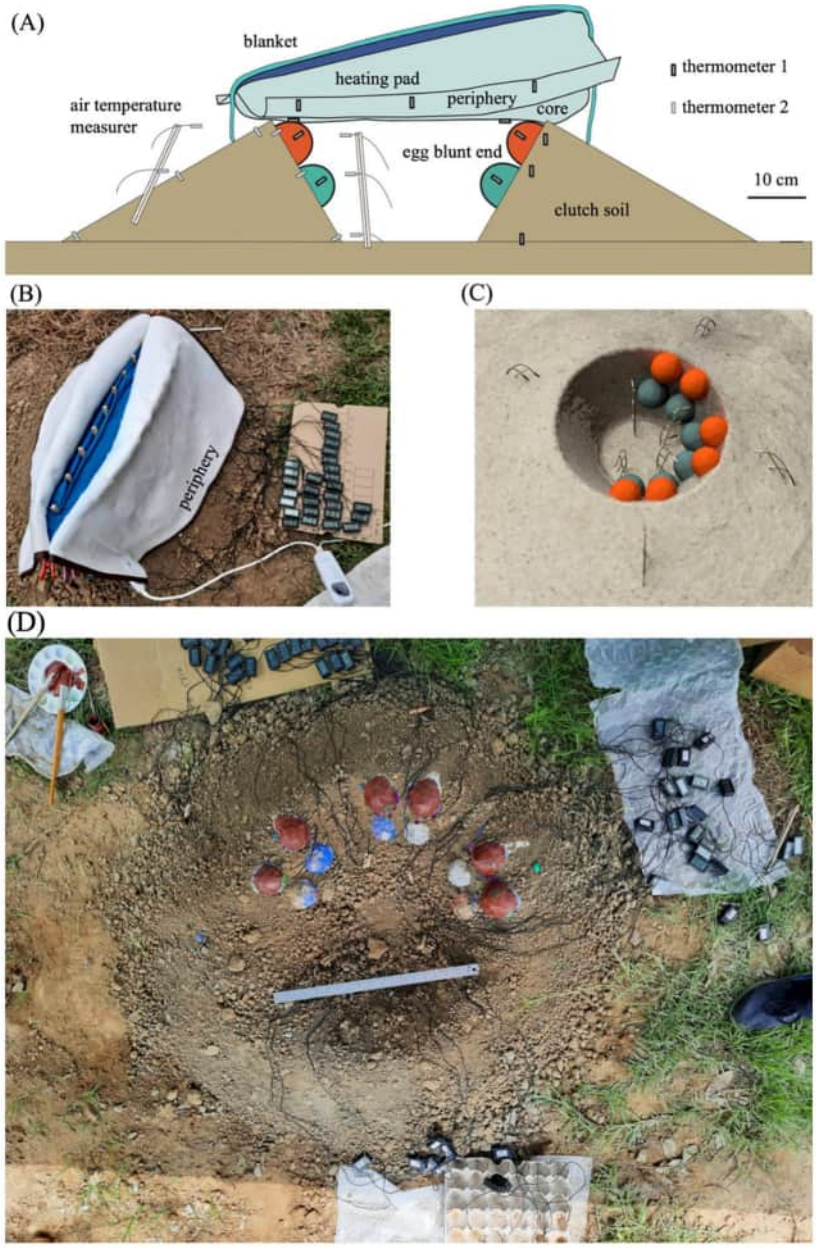

FIGURE 3
The design of the incubation experiments. **(A)** The arrangement of thermometers in the incubation experiments. Thermometers 1 (with thicker outlines) were used in Experiment II. Thermometers 2 (with lighter outlines) were the additional thermometers used in Experiment III. The schematic presents a lateral view of the clutch and the incubator. **(B)** The actual setup of Experiment II (without blanket). The thermometers were collectively placed on labeled cardboard. Pictures of the readings of the thermometers were taken during data collection. **(C)** A computer-rendered graphic depicting the arrangement of air temperature measurers in Experiment III. There were four measurers inside the clutch and three outside. The ones inside measured air temperature at heights of 0 cm, 12 cm, and 18 cm above the ground. The ones outside measured air temperature at heights of 12 cm and 18 cm above the ground. The red eggs represent the outer-ring eggs, whereas the green eggs represent the inner-ring eggs. **(D)** A photograph of the generalized clutch after Experiment III.

performed under the environmental conditions of Experiment II and Experiment III with COMSOL Multiphysics 6.1.

The posture simulations were designed to closely match the settings of the two experiments. Eggs were assigned different contact areas based on measured values. Contact temperatures from the incubator closest to each egg, either derived from measurements at the core or the periphery, were applied to the corresponding contact areas to represent the incubation temperature. These simulations were used to verify the temperature distribution trends observed in Experiment II and Experiment III.

In the non-posture simulations, extreme scenarios were created based on the experimental data. The maximum recorded contact area and contact temperature were applied to all outer-ring eggs. The homogeneous setting minimized the influence of the adult's

posture over the eggs to help examine the effects of heat sources other than the incubator, such as the sun, on the temperature distributions within the clutch.

2.2.2 Model geometry

The simulated clutch replicated the dimensions of the generalized clutch and was built in the COMSOL Multiphysics model builder. The below-ground soil was modeled as a cylinder with one meter in both the diameter and the depth.

A two-dimensional oviraptorid egg shape was rotated along its longest axis to form a three-dimensional oviraptorid egg. It was offset to form two bodies, generating an outer layer (the shell) and the inner layer (the egg white). The outer layer had the same dimension as NMNS CYN-2004-DINO-05 described in Wiemann et al. (2017). The inner layer was 1.8 mm less along each boundary compared to the outer layer, creating a space between the two layers that represented the eggshell with a thickness of 1.8 mm, a value derived from the eggshell of *Macroolithus yaotunensis* (Yang et al., 2019b; Weiß, 2020). The shell was assigned chicken eggshell material properties. The inner layer was assigned chicken albumen material properties.

The clutch rim had a right-triangular lateral view. The inner wall was tilted 60° relative to the ground while the outer wall was tilted 30° relative to the ground (Figure 4). All eggs were arranged as they were in the generalized clutch, with the only difference that the central angle between the eggs within a pair was 30° instead of 20° as in the experiment because of the limiting drawing capacity of the software.

In the posture simulations, the blunt ends of the eggs were sliced to match each egg's respective contact area. When simulating Experiment III, an area of 15 cm^2 of the clutch was sliced next to egg 6-o to represent the position where the incubator contacted the soil. In the non-posture simulations, however, every egg was sliced uniformly to have the maximum recorded contact area. Free tetrahedra were used for meshing.

2.2.3 Boundary conditions

In the model, the incubator was not drawn. Instead, the incubator's contact temperatures (T_c) were applied to the slices that matched the measured contact area of the eggs (Figure 4). The values of T_c varied based on the position of the egg (core or periphery). For posture simulations with the environmental settings of Experiment II, T_c were the average temperatures of either the core or the periphery over the last seven hours (16:02-23:02) of the experiment. T_c of 36.4°C was assigned to egg 1-o, 2-o, and 6-o, whereas a T_c of 32.3°C was assigned to egg 3-o, 4-o, and 5-o. For simulations with the environmental settings of Experiment III, T_c was assigned as the linearly interpolated functions of the recorded incubator core or periphery temperatures because the incubator temperature had diel fluctuation.

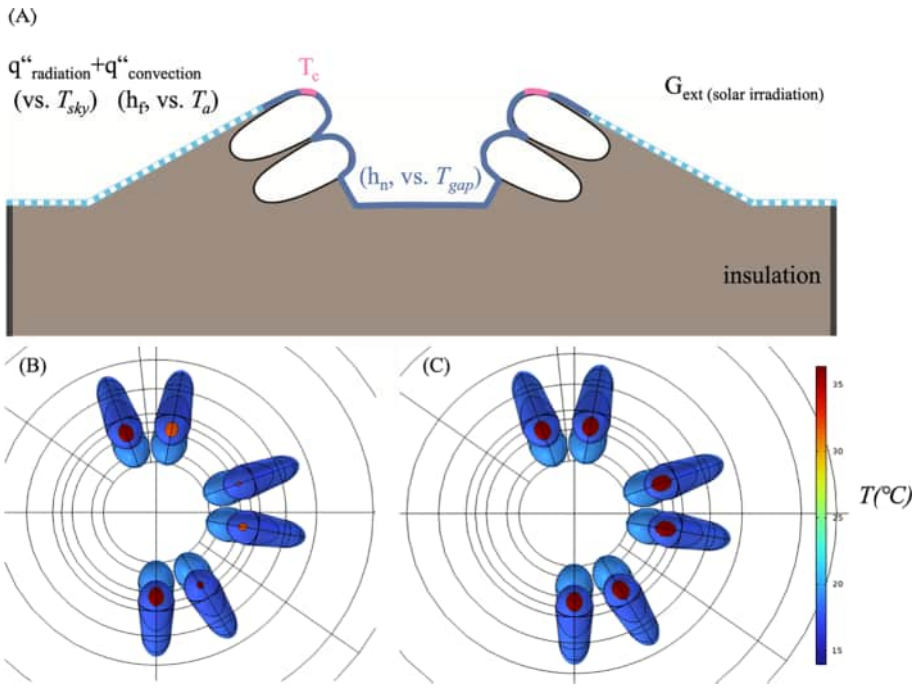

FIGURE 4
(A) Boundary conditions of the posture simulations and the non-posture simulations. **(B)** The initial temperatures of the posture simulation of Experiment II. **(C)** The initial temperatures of the non-posture simulation of Experiment II. Both kinds of simulations have contact temperatures (T_c, indicated by the pink lines), solar radiation (G_{ext}) and heat flux ($q"_{radiation}$ and $q"_{convection}$) on the exterior clutch wall and the ground (indicated by the dashed light blue lines), soil insulation (indicated by the dark-gray lines), and convective heat flux of natural convection within the clutch (h_n vs. T_{gap}, indicated by the dark blue lines). The differences between the posture and the non-posture simulations lie in their contact area and contact temperature T_c. For posture simulations, the contact area and posture vary according to the experimental records **(B)**. The non-posture simulations have uniform contact area and contact temperature **(C)**.

In all simulations, forced convection (h_f) (e.g., blown by the wind) was applied to the exterior of the clutch. The surrounding temperature for parameterizing h_f was based on the ambient temperature data from the meteorological station G2F820 (Ta) (Figure 4A). Convective heat flux of natural convection in the air (h_n) was applied to the surface of the eggs and of the soil inside the clutch (Figure 4A). The surrounding temperature for h_n was based on the measured air gap temperature (T_{gap}) at different positions inside the clutch. The convective heat transfer coefficient (h) of the heat flux was calculated based on a simplified geometry.

Surface-to-ambient radiation was applied to account for solar radiation and the radiation between the ground and the sky. Since the clutch was covered by the incubator and the feathers during the experiment, the sun (G_{ext}) only radiated to the ground and up to 12 cm above the ground on the exterior clutch wall, and the same area radiated to the sky (G_{amb}) (Figure 4A). Radiation within the clutch was not considered since heat conduction was the dominant mechanism of heat transfer due to a low temperature difference between the incubator and the eggs. Additionally, calculating radiation among irregular shapes constructed by the incubator and the inner side of the clutch would require a substantial computational power that is beyond our capacity and defeat a simulation's purpose of simplifying a real-world context. Thermal insulation was applied on the side of the soil cylinder. The bottom of the soil cylinder was assigned the soil temperature measured one meter underground by the meteorological station (Figure 4A).

2.2.4 Materials and parameters

The thermophysical properties implemented in the simulations were acquired from measurements, literature review, and the material library of COMSOL Multiphysics. When calculating thermal conductivity of the soil, it was assumed that the local soil had a quartz (SiO2) content of 0.9, the same as loamy sand (Tarnawski et al., 2011). The thermal properties of the air were calculated using the relationship described in McQuillan et al. (1984). The thermal properties of the oviraptorid eggs were assumed to be the same as chicken eggs, with the chicken eggshell material property assigned to the eggshell and the chicken egg white material property assigned to the egg white in the model. Egg yolk was not represented in the model. The values and the sources of the properties were shown in Table 1.

Since the ambient temperature had a small range in the experiments, the thermal properties of the air at its average temperature were used to calculate the dimensionless Grashof number (Gr), the Prandtl number (Pr), and the Rayleigh number (Ra) to derive the Nusselt Number (Nu), which was then used to calculate the convective heat transfer coefficient (h) (Incropera et al., 2006). Weather data of the average wind speed over the experimental period were retrieved from the meteorological station G2F820. When calculating forced convection, the wind speed was assumed to be the same as the average wind speed over the experimental period. For posture simulations that required assigning convective heat transfer coefficients (h), the clutch was simplified into basic geometries which had known relations between the dimensionless numbers and Nu because of a lack of research on the convective heat transfer coefficient of objects similar to an oviraptorid clutch. Geometries used for calculating h for laminar flow included: a sphere for the blunt end of the egg, an inclined plate for the interior clutch wall and part of the exterior clutch wall, and a horizontal plate for the center devoid of eggs. The sphere had a diameter equal to the average of the major and the minor axes of the blunt end. The interior clutch wall had a characteristic length of 0.192 m, while the upper part of the clutch wall was 0.075 m. Nu and h were calculated from the correlations of these geometries. The lower exterior clutch wall and the rest of the surface exposed to the environment were assumed to have the same correlation as a flat plate in turbulent flow (Kumar and Mullick, 2010).

The emissivity of the soil (ε_{soil}) was assumed to be 0.975, the same as sandy soil (Mira et al., 2007). Hourly total solar irradiance (MJ/m^2)

TABLE 1 Material properties used in the simulations.

Material type	Density (kg/m^3)	Thermal conductivity ($W/m{\cdot}K$)	Heat capacity ($J/kg{\cdot}K$)	Source
Soil	1460	Soil moisture 0.07 (mL/cm^3): 0.793 Soil moisture 0.05 (mL/cm^3): 0.488	Soil moisture 0.07(mL/cm^3): 968.89 Soil moisture 0.05 (mL/cm^3): 926.31	Calculated from Yang et al. (2005)
Chicken Eggshell	2241	2.25	888	Carter (1968), Denys et al. (2003)
Resin Eggshell	1350 (under 28.2°C)	0.22	1280 (under 24.00 °C)	Measured with Laser Flash Thermal Diffusivity Analysis, Differential Scanning Calorimeter, True Density Analyzer
Egg White (under 25 °C)	1040.45	0.5449	3800	Abbasnezhad et al. (2016)
Water	Temperature Dependent	Temperature Dependent	Temperature Dependent	COMSOL Materials
Air	$\frac{351.99}{T}+\frac{344.84}{T^2}$	$\frac{2.3340\times10^{-3}\times T^{\frac{2}{3}}}{164.54+T}$	$1030.5 - 0.19975\ T + 3.9734 \times 10^{-4}\ T^2$	McQuillan et al. (1984), COMSOL Materials

was acquired from the meteorological station G2F820 and converted to the hourly average solar irradiation, Gext (W/m^2), for the simulations. The ambient temperature to which the soil emits radiation, the effective sky temperature, T_{sky}, was derived by first calculating the sky emissivity (ε_s) using the dew point temperature and the ambient air temperature (T_a) acquired from the meteorological station (Berdahl and Fromberg, 1982), then using Equation 2 to estimate the effective sky temperature (Gliah et al., 2011).

$$T_{sky} = (\varepsilon_s * T_a^4)^{1/4} \quad (2)$$

Surface to ambient radiation was applied on the soil surface as Equation 3:

$$G_{ext} = \varepsilon_{soil}(T^4_{soil,surface} - T^4_{sky}) + h_f(T_{soil,surface} - T_a) \quad (3)$$

The soil was assumed to be an opaque medium, where the absorptivity and the emissivity of the soil surface were assumed to be corresponding to a diffuse surface. The ambient was approximated as a blackbody at the effective sky temperature.

2.2.5 Governing equations

For heat transfer in solids, the transient heat transfer is governed by conduction as in Equation 4:

$$\rho C_p \frac{\partial T}{\partial t} + \nabla \cdot (\vec{q}) = Q_{total} \quad (4)$$

where

$$\vec{q} = -k \nabla T \quad (5)$$

In Equations 4 and 5, ρ is density of the material (kg/m^3), C_p is the heat capacity under constant pressure (J/(kg·K)), T is the absolute temperature (K), $\vec{q}$ is the heat flux (W/m^2), k is the thermal conductivity, Q_{total} is the heat source in solid (W/m^3).

2.2.6 Initial values

The average of the temperatures of the eggs in the same ring at the start of the experiments was assigned as the initial egg temperature for eggs in that specific ring. Soil temperature within the raised clutch rim was taken directly from the measurements. For the underground soil, temperature data were obtained from the meteorological station G2F820. Since the above-ground rim raised the soil temperature below it, the soil temperature measured at the depths of 20 cm underground and below were assigned to the soil with depths 20 cm above that of the measured depth in the simulation (e.g., 30 cm becomes 10 cm underground). For soil deeper than 50 cm, the soil in the simulation had the same temperature as that recorded by the meteorological station G2F820. The initial temperature of the air-gap air in the non-posture simulation was a linearly interpolated function with respect to the z-axis that reflects the temperature of the nearby soil.

2.2.7 Study

The model was time-dependent. For the simulations replicating Experiment II and Experiment III, the overall simulated time was 900 and 1,800 minutes, respectively.

3 Results

3.1 Incubation experiments

3.1.1 Experiment I: no incubator

At the onset of the experiment, the inner-ring eggs generally had higher initial temperatures than the outer-ring eggs, with a mean difference of 1.2°C (29.0°C vs. 27.8°C). As the experiment progressed, the mean temperature of all eggs rose from 28.2°C to 42.0°C at time 13:26, with egg 1 reaching 46.0°C. Between corresponding outer- and inner-ring eggs—for instance egg 2 and 12, and egg 3 and 13—the outer-ring eggs had lower maximum temperatures than the inner-ring eggs. For egg 1 and 11, however, the outer-ring egg 1 had a higher maximum temperature.

The shaded ambient temperature ranged from 23.2°C to 30.8°C during the experimental period. Overall, the ambient temperature, the eggs, and the soil had similar temperature profiles. They all reached their maximum temperature at around 13:26 and declined thereafter. The egg temperature varied more than either soil temperature or shaded ambient temperature. The temperature difference experienced by an individual egg ranged from 11.3°C in egg 3 to 18.3°C in egg 1.

3.1.2 Experiment II: incubator in a colder environment

In this experiment, the incubator contacted none of the inner-ring eggs. Among the outer-ring eggs, egg 1-o was most contacted, with an area of 12.32 cm^2. The least contacted egg was egg 4-o, with an area of 0.76 cm^2.

The inner-ring eggs had a higher initial average temperature than that of the outer-ring eggs, 19.1°C and 17.5°C respectively. As the experiment progressed, the core outer-ring eggs, egg 1-o, 2-o, and 6-o, reached equilibrium at 17:02 and stayed within ± 0.2°C (Figure 5). Comparing the average temperature over the final four hours (19:22-23:02) of the experiment of these three eggs, egg 1-o

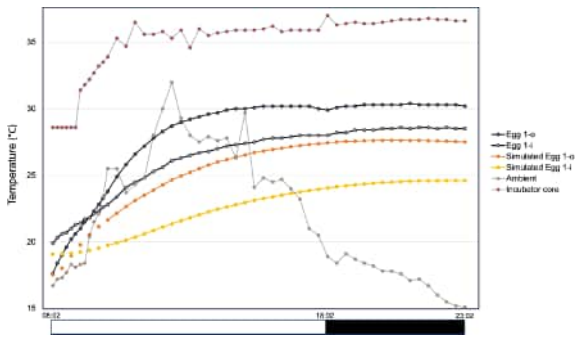

FIGURE 5
The temperature profiles of Experiment II and a selected set from posture simulation for Experiment II. The temperature profile of the incubator core, egg set 1, and the ambient temperature of Experiment II are shown in dark colors. The simulated temperature profile of egg set one is shown in warm and bright colors. Aside from some peripheral eggs showing a decline in temperature at the end of the experiment, most eggs have temperature profiles similar to those of egg set 1.

10.3389/fevo.2026.1351288

had the highest value of 30.3°C, followed by 28.0°C for egg 6-o, and 25.7°C for egg 2-o. For the peripheral outer-ring eggs, egg 3-o, 4-o, and 5-o, their temperatures declined gradually after sunset at 17:42 and reached lower equilibrium temperatures than the core outer-ring eggs. Their average temperatures over the final four hours of the experiment were 25.6°C of egg 3-o, 25.1°C of egg 5-o, and 24.4°C of egg 4-o. The inner-ring eggs reached equilibrium about three hours later than the corresponding outer-ring eggs in the same set. Contrary to their outer-ring counterparts, the temperatures of eggs 3-i, 4-i, and 5-i did not decline. The average temperatures over the final four hours of the inner-ring eggs were 28.5°C for egg 1-i, 26.3°C for egg 2-i, 24.7°C for egg 3-i, 23.7°C for egg 4-i, 25.1°C for egg 5-i, and 25.8°C for egg 6-i.

The soil and the eggs had similar temperature profiles. The temperatures of the inner-ring eggs were approximately the same as those of the surrounding soil, while the outer-ring eggs had temperatures higher than those of the surrounding soil.

At the end of the experiment, the maximum temperature difference within the outer ring was 6°C between egg 1-o and egg 4-o (30.2°C vs. 24.2°C). The maximum temperature difference within the inner ring was 3.8°C between egg 1-i and egg 4-i (28.5°C vs. 23.7°C). All egg temperatures were well above the ambient air temperature.

Zooming in on the comparison between sets, it was observed that in the core sets, the outer-ring eggs had higher average temperatures over the final four hours than the inner-ring eggs. For example, in set 1, egg 1-o was 1.8°C higher than egg 1-i. In the peripheral sets, the differences were much smaller. For instance, in set 4, egg 4-o was 0.7°C higher than egg 4-i (Figure 6A1). In set 5, the average temperature was the same, and the temperature of egg 5-o fell below that of egg 5-i by 0.6°C by the end of the experiment. Moreover, the core sets generally had higher equilibrium temperatures than the peripheral sets. The results showed two general trends: (a) the closer a set was to the core, the larger the

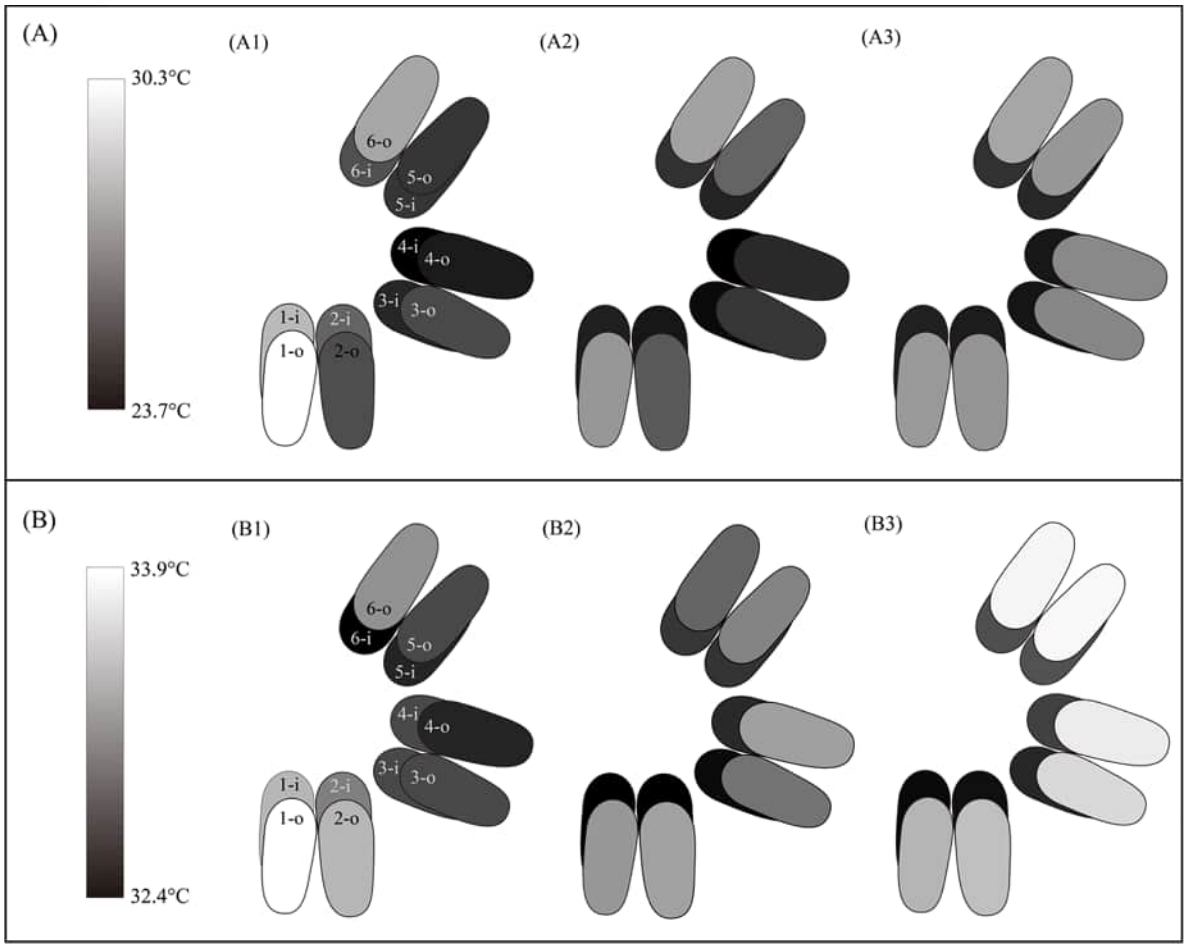

FIGURE 6
(A1) The average blunt-end temperatures of the eggs over the final four hours of Experiment II. The average equilibrium temperature of each egg over the final four hours of the experiment is converted to different colors, with black indicating the coldest and white the hottest. **(A2)** The average blunt-end temperatures of the eggs over the final four hours of the posture simulation of Experiment II. **(A3)** The average blunt-end temperatures of the eggs over the final four hours of the non-posture simulation of Experiment II. **(B1)** The average blunt-end temperature of each egg over the 24-hour period of Experiment III. **(B2)** The average blunt-end temperature of each egg over the 24-hour period of the posture simulation of Experiment III. **(B3)** The average blunt-end temperature of each egg over the 24-hour period of the non-posture simulation of Experiment III.

temperature difference between the inner- and outer-ring eggs was; (b) the closer an egg was to the core, the higher its equilibrium temperature was (Figure 6A1).

The highest equilibrium temperature over the final seven hours of the experiment was observed in egg 1-o (30.2°C), whereas the lowest was in egg 4-i (23.4°C). The average ambient air temperature over the final seven hours was 18.9°C; the average incubator temperature over the same period was 36.4°C. Calculating from Equation 1, the estimated oviraptorid adult incubation efficiency was 26%~65%.

3.1.3 Experiment III: incubator in a hotter environment

As in Experiment II, the incubator contacted none of the inner-ring eggs. Among the outer-ring eggs, egg 4-o was most contacted, with a contact area of 10.2 cm^2. Egg 3-o was least contacted, with a contact area of 5.3 cm^2. Egg 1-o and 2-o were contacted by the core, egg 3-o, 4-o, and 5-o were contacted by the periphery, and egg 6-o was not contacted (Please refer to Figure 2A for egg arrangement in the clutch).

The partial clutch heated directly by the sun showed extreme temperature fluctuations. The outer-ring egg reached its maximum temperature of 54.1°C at 14:13. The inner-ring eggs had lower maximum temperatures, which were still higher than the unshaded ambient temperature. At night, the lowest temperature of the outer-ring egg was 26.4°C, which was still higher than the ambient temperature at that time. The outer-ring egg had a higher maximum and a lower minimum temperature than the inner-ring eggs, with a maximum temperature difference of 27.6°C.

Due to pre-heating, the initial temperature of the incubator core was 39.6°C, but this value soon dropped to 36.5°C after 40 minutes and maintained a mean of 37.1°C for the rest of the experiment. For the incubator periphery, the temperature was more unstable. It first rose from its initial value of 34.4°C to 41.5°C at 14:13, and then declined to 32.5°C at 18:53. It maintained around 32.8°C until 06:33, then rose again at dawn, reaching 41.6°C at 12:53 of the second day.

For the generalized clutch, the egg temperatures had diel fluctuations (Figure 7). The maximum and minimum temperatures appeared later in comparison to the ambient temperature, resembling a phase shift. All outer-ring eggs had higher maximum temperatures and lower minimum temperatures than the inner-ring eggs, with a temperature range of 5.2°C for egg 1-o and 3.5°C for egg 1-i over the 24-hour period (12:13, July 25 to 12:13, July 26). Moreover, egg sets closer to the core reached their maximum temperature about an hour earlier than the eggs at the periphery. In addition to the difference in timing, the core eggs had a lower maximum temperatures and higher minimum temperatures than the peripheral eggs (e.g., egg 2-o had 36.2°C for the maximum temperature while egg 4-o had 37.4°C; egg 2-o had 30.6°C for the minimum temperature while egg 4-o had 30.4°C). The average egg temperature over the 24-hour period was higher at the core (33.1°C for egg 1-o and 32.8°C for egg 6-o) than at the periphery (32.5°C for egg 4-o; Figure 6B1). For the average temperature difference

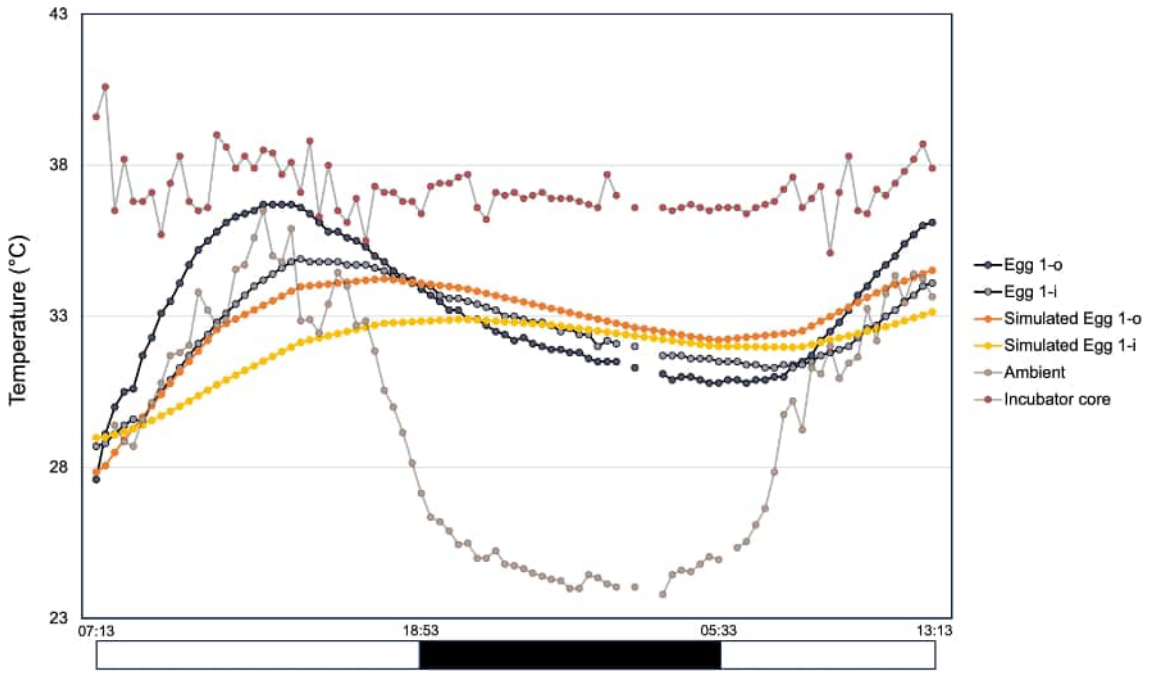

FIGURE 7
The temperature profiles of Experiment III and a selected set from posture simulation for Experiment III. The temperature profile of the incubator core, egg set 1, and the ambient temperature of Experiment III are shown in dark colors. The simulated temperature profile of egg set 1 is shown in warm and bright colors. Egg set 1 demonstrates the diel fluctuation of the egg temperatures, with the outer-ring egg having a higher maximum and a lower minimum temperature than the inner-ring egg.

between the outer- and inner-ring eggs (outer minus inner) within the same set, the trend that core sets had higher temperature differences than the peripheral sets was also observed. In some sets, such as set 4, the difference was slightly negative.

Soil temperatures also had diel fluctuations. Generally, the higher the soil was above the ground, the higher its maximum and the lower its minimum temperature were. Among the surface soil of the exterior clutch wall, the soil covered by the blanket had much lower temperature than sites that were not, with more than 10°C difference in the maximum temperature. The lowest maximum temperature of the surface soil of the exterior clutch wall exceeded 40°C. Some, such as those not covered by the blanket, reached as high as 57.6°C.

3.2 Heat transfer simulation results

3.2.1 Simulations for Experiment II

3.2.1.1 Posture simulation

The simulated results showed good agreement with the experimental trends (Figure 6A2). As in the experiment, the temperature of the eggs increased and stabilized in the final few hours of the simulation. A pattern was observed in which the closer an egg was to the periphery, the lower its equilibrium temperature became: the core egg 1-o reached an equilibrium (final four hours) temperature of 27.6°C, whereas the peripheral egg 4-o had the lowest temperature at 24.8°C. The egg temperatures increased as the position of the egg approached the incubator core from the periphery, with the core egg 6-o exhibiting the highest equilibrium temperature of 27.9°C (Figure 6A2). The inter-ring temperature difference of the final four hours of the simulation also showed a similar trend. Egg 1-o was 3.1°C warmer than egg 1-i, and egg 6-o was 2.9°C warmer than egg 6-i, whereas egg 4-o was only 0.8°C warmer than egg 4-i. (Figure 6A2; see also Supplementary Figure S3 for the final temperature distribution of the simulation and Supplementary Video S2 for the animation for the simulation for posture simulation for Experiment III).

3.2.1.2 Non-posture simulation

The inter- and intra-ring temperature distribution patterns were largely absent in the non-posture simulation of Experiment II. Core outer-ring eggs, such as egg 1-o (27.7°C), had slightly higher average equilibrium temperatures than some peripheral eggs, such as egg 3-o and egg 4-o (27.2°C). The inter-ring temperature differences were similar across sets, with the core sets, such as set 2 (3.1°C), having slightly higher temperature differences than the peripheral sets, such as set 4 (2.9°C) (Figure 6A3).

3.2.2 Simulations for Experiment III—

3.2.2.1 Posture simulation

As in the experiment, egg temperatures exhibited diel fluctuations and the outer-ring eggs reached higher maximum temperatures. Some inner-ring eggs, such as eggs 1-i, 2-i, and 3-i, reached lower minimum temperatures than some outer-ring eggs, such as eggs 1-o and 2-o. Regarding the temperature trend, the intra-ring temperature pattern observed in the experiment was absent. For the average outer-ring temperature over the 24-hour period, eggs 1-o, 2-o, and 4-o shared the highest value of 33.3°C, whereas egg 6-o had the lowest value of 33.0°C. Regarding the inter-ring temperature variation, the temperature differences in the core sets were slightly larger than the sets closer to the periphery (e.g., the difference in set 2 was 0.5°C greater than the difference in set 5). However, set 6 had the minimum difference of 0.3°C (Figure 6B2; see also Supplementary Figure S3 for the final temperature distribution of the simulation and Supplementary Video S2 for the animation for the simulation for posture simulation for Experiment III).

3.2.2.2 Non-posture simulation

The outer-ring eggs had almost uniform temperatures, with a maximum difference of 0.4°C between egg 1-o (33.5°C) and 5-o (33.9°C). The average outer-ring egg temperatures increased almost incrementally from egg 1-o to egg 6-o. The average inter-ring temperature difference was nearly uniform (0.7°C), except for set 1, which was 0.3°C higher than the average (Figure 6B3).

4 Discussion

4.1 The equations for incubation efficiency

Overall, the incubation efficiency obtained in this study is robust across various calculation methods. The incubation efficiency range obtained using Hogan and Varricchio (2021)'s equation, with the maximum incubator temperature being 37°C and the minimum ambient temperature being 15.1°C, is 20.5%-51.5%. This range is similar to that of 26%-65% obtained through our equation and yields a similar interpretation of oviraptorid brooding behavior, supporting the comparability of our results (Hogan and Varricchio, 2021).

An extension of Equation 1 involves integrating the difference between egg temperature and ambient temperature over time and dividing this integral by the integral of the difference between incubator temperature and ambient temperature. This extension evaluates the contribution of the incubator to elevating egg temperature above fluctuating ambient temperatures when the egg temperature does not reach equilibrium, making it especially suitable for eggs experiencing diel temperature fluctuations, such as those in Experiment III. Using the trapezoidal method to approximate the integrals, the resulting incubation efficiency for Experiment II ranges from 26% to 65%, whereas the incubation efficiency for the final 24-hour period of Experiment III ranges from 49% to 55%. The identical incubation efficiency range for Experiment II supports the validity of this approach. The resulting incubation efficiency for Experiment III falls within a comparable range to that of Experiment II and suggests similar incubator efficiency in both hotter and colder environments.

One limitation of all methods for calculating incubation efficiency discussed above is the difficulty in delineating the contributions between the incubator and other environmental heat sources on egg's temperatures. The incubation efficiency is

calculated under the assumption that the ambient heat source has similar thermal effects on the ambient air temperature and the clutch. In the equation, the ambient air temperature is treated as the basis for no thermal influence from the incubator and subtracted to accentuate the influence of the incubator on the eggs when the effects of the environmental heat are accounted for. However, this assumption may not be realistically accurate, as soil usually heats up to a higher temperature than the ambient air temperature, and the eggs were heated up directly by the soil rather than the ambient air. As such, the presence of a strong environmental heat source, such as the sun, may bias the calculated efficiency.

A more accurate method for assessing the thermal effects of the incubator on elevating the egg's temperature above that of the ambient is to measure the temperature of the eggs when the incubator is present but provides no heat. A replica of the same experimental setup that runs in parallel to the main experiment can achieve the comparison and provide a more accurate basis than the ambient air temperature. However, due to logistical constraints, such a plan was not implemented. Alternatively, simulations that accounts for solar irradiation but excludes the heat of the incubator can be performed in a similar manner to the simulations implemented in this study and provide a more accurate basis for calculating incubation efficiency. Future investigations into the appropriate equation quantifying the incubating adult's contribution to the eggs will greatly benefit the field.

4.2 Heat transfer within an oviraptorid clutch

4.2.1 Temperature distribution patterns

Egg temperatures stabilized in the final few hours of Experiment II but did not do so in Experiment III. The difference can be explained by the sun acting as an additional, powerful heat source in Experiment III.

The solar effect in Experiment II was not as powerful as in Experiment III. Even though the air and the soil temperatures in Experiment II displayed diel fluctuations, they remained below the incubator temperature. Thus, the air and soil acted as heat sinks, whereas the incubator acted as a heat source. Over time, the eggs reached temperatures between the ambient and incubator, consistent with the results reported by Hogan and Varricchio (2021) and Hogan (2024).

In Experiment III, nevertheless, the sun raised the temperatures of the soil along the exterior clutch wall well above that of the incubator during the day. Instead of acting as a heat sink, the soil, alongside the incubator, heated up the eggs and raised their temperatures. After sunset, when the ambient temperature fell below the egg temperature, the air and surrounding soil again functioned as heat sinks, producing the pronounced diel fluctuations observed in Experiment III.

Despite the differences in temperature profiles, both experiments showed consistent temperature distribution patterns: (1) The core outer-ring eggs had higher average temperatures than the peripheral outer-ring eggs. (2) The temperature differences between the outer- and inner-ring eggs were larger in core sets than in peripheral sets. These patterns were also present in the posture simulation of Experiment II, but they were less pronounced in the posture simulation of Experiment III. More detailed initial conditions for the simulation may help reproduce the small temperature differences observed in Experiment III.

It should be emphasized that the above generalizations are based on a clutch with 12 eggs. An oviraptorid clutch could contain 10 pairs (20 eggs) or more, which could have yielded very different results. Furthermore, caution is warranted against overgeneralizations since this study was designed based on specific interpretations of oviraptorid behaviors and physiology for clutches of a specific size class. We thus refrain from applying the interpretations to a general condition and instead limit our discussions to the incubator model and clutches built for this study.

4.2.2 The major contributor to the temperature distribution patterns

Comparing the posture and the non-posture simulations of Experiment II, it can be observed that the abovementioned temperature distribution patterns are much more pronounced in the posture simulations but to a lesser extent in the non-posture simulations, which by design excluded the effects of different contact areas and temperatures due to the adult's posture. Since both types of simulations experienced the same time-dependent solar radiation specific to the experimental settings, solar radiation may contribute to the observed patterns much less than the adult's posture. As the incubator and the sun were the only two heat sources in the system, by deduction, the adult's posture is most likely the major contributor to the patterns.

The variations in incubation temperature within the reconstructed clutch resulting from the adult's position may have been caused by unequal contact areas and temperatures, as well as by differing rates of heat loss. As observed in the experiments, the incubators had unequal contact areas with the eggs. In extant bird nests, such a condition may arise when many eggs crowd the nest, causing some eggs to be only partially contacted and therefore receive less heat from the brooding adult (Bortolotti and Wiebe, 1993). Additionally, peripheral eggs may experience higher rates of heat loss. In extant birds, eggs located nearer the periphery are more exposed to the environment and cool more rapidly when the incubating adult is absent (Boulton and Cassey, 2012). Our interpretation of inter-ring temperature variation as being caused by differences in contact area potentially provides an explanation for the inter-ring temperature variation observed in Hogan (2024), despite the paper's unrealistic radially symmetric design of the incubator. Importantly, however, if our incubator model had been capable of movement, the temperature differences described above might not have been as pronounced.

4.3 Oviraptorid reproductive biology

4.3.1 Incubation temperature and embryonic development

If the embryos of insects, turtles, and lizards are not incubated at extremely high or low temperatures, their development rates have

positive linear relationships with the incubation temperature (Wagner et al., 1984; Georges et al., 1994, 2005). Based on the avian developmental temperature range of 26°C to 40.5°C (Conway and Martin, 2000), it is reasonable to assume that the recorded incubation temperatures of 30.4°C to 37.4°C over the 24-hour period (12:13, July 25th to 12:13, July 26th) of Experiment III do not approach the extremes of oviraptorid developmental temperature.

4.3.2 Environmental heat sources and embryo vitality

While some paleontologists hypothesize that the adult-clutch association primarily served to protect eggs from predation (Norell et al., 1995; Dong and Currie, 1996; Deeming, 2002; Yang et al., 2019b), shielding eggs from external environmental stressors, such as sunlight, may also have driven the evolution of oviraptorid incubation behavior. Our experiments suggest that solely relying on ambient heat sources for incubation would have increased embryonic mortality due to exposure to lethal incubation temperatures. Unlike Argentinian sauropods, there is no evidence that oviraptorosaurians utilized geothermal heat to incubate their eggs (Grellet-Tinner and Fiorelli, 2010). If ambient heat came only from solar radiation and an oviraptorid clutch was left unattended, the eggs in the partially open nest would have experienced extreme diel temperature fluctuations that reduced hatching success. For avian embryos, exposure to temperatures above 41°C for several hours leads to mortality (Webb, 1987). In the experiments, some eggs reached 46°C in Experiment I and 54.1°C in the partial clutch of Experiment III. In both cases, the egg temperatures remained above 41°C for more than four hours. As oviraptorid embryos exhibit several avian features and may have physiology similar to that of precocial birds (Norell et al., 2001; Grellet-Tinner and Makovicky, 2006; Weishampel et al., 2008), it is likely that oviraptorid embryos cannot withstand the extreme environmental conditions under direct solar exposure. Moreover, birds that expose eggs to sunlight before clutch completion, such as ostrich (*Struthio camelus*), have eggs with white eggshell, which absorb less heat compared to the colored ones, and a larger volume that confers greater heat capacity (Bertram, 1992). By comparison, oviraptorid eggs are smaller and contain blue-green pigmentation, potentially making them more vulnerable to overheating under solar exposure than ostrich eggs (Downs and Ward, 1997).

Shielding the eggs from extreme temperature fluctuations may also have benefited embryonic survival. Without the incubator, the egg temperatures dropped substantially at night, sometimes by more than 20°C, as recorded in the partial clutch. The magnitude of fluctuation is far greater than that observed in crocodile nests, where egg temperatures are maintained within 3°C (Magnusson, 1979). For avian embryos, the continuous fluctuation between the optimal developmental temperature and the physiological zero, the temperature above which the embryos begin to develop (Lundy, 1969; Webb, 1987), may impair development (Stoleson and Beissinger, 1995). Although unincubated embryos have a broader thermal tolerance and are better at surviving temperatures below the physiological zero (Booth, 1987; Stoleson and Beissinger, 1995), previous experiments have shown that no ostrich embryo survives after 15 days of outdoor exposure (Bertram and Burger, 1981).

Due to the risk of reducing embryonic survivorship, oviraptorids probably would not have left their eggs exposed to the environment without care for an extended period. Adult clutch attendance likely assisted embryonic development by reducing the extreme temperature variation and preventing eggs from experiencing lethal incubation temperature (Norell et al., 1995), an adaptation also observed in modern birds (Wang and Beissinger, 2011). Such an interpretation complicates Hogan (2024)'s hypothesis on the role incubation plays in subaerial nesting strategies, as the brooding adult may have regulated clutch temperature against large-magnitude fluctuations in addition to conferring thermal advantages beyond environmental heat sources.

4.3.3 The temperature distribution patterns and asynchronous hatching

4.3.3.1 Intra-ring asynchronous hatching

Intra-ring temperature variation within the outer ring has been reported by Bi et al. (2021), with differences ranging from 4°C to 8°C. In Experiment II, the maximum temperature difference within the outer ring was 6°C, which may have contributed to intra-ring asynchronous hatching. In ostriches, eggs incubated continuously at 37.5°C hatch, on average, in 39.3 days (Hassan et al., 2004), whereas reducing the incubation temperature to 35°C extends the mean incubation period to 47 days (Hoyt et al., 1978). With a higher incubation temperature, the core outer-ring eggs may have developed faster than the peripheral outer-ring eggs.

In Experiment III and its associated simulations, however, the greatest difference between the 24-hour average temperature of the outer-ring eggs was 0.6°C. This result is inconsistent with the profound temperature difference of the adult-associated clutch discovered in the Nanxiong Group (Bi et al., 2021). The less profound temperature difference suggests that oviraptorid eggs may not have exhibited intra-ring asynchronous hatching in a hotter environment if outer-ring eggs were laid almost concurrently.

4.3.3.2 Inter-ring asynchronous hatching

The reproductive constraints imposed by oviraptorid clutch structure likely shaped the early development of inner-ring eggs. With the highly organized egg pairs being partially buried in the clutch sediment (Clark et al., 1999; Wiemann et al., 2017), the oviraptorid adults were unlikely to discard the early-laid, less viable eggs in the manner seen in ostriches (Bertram, 1992). To avoid reducing the viability of unattended eggs, oviraptorids may have shaded the eggs, as seen in ostriches (Bertram, 1992), incubated the eggs partially (at lower intensity before clutch completion; Wang and Beissinger, 2011), as in emus (*Dromaius novaehollandiae*) (Buttemer et al., 1988), or incubated the eggs fully (Stoleson and Beissinger, 1995; Wang and Beissinger, 2011). As either high ambient temperature or incubation before clutch completion can initiate early development of the embryos (Grenier and Beissinger, 1999; Griffith et al., 2016), it is very likely that the inner-ring eggs began developing prior to the outer-ring eggs (Yang et al., 2019a).

In a colder environment similar to that experienced by *Nemegtomaia* in the Nemegt Formation, the core outer-ring egg may have hatched earlier than the core inner-ring egg, whereas the peripheral outer-ring egg may have hatched later or at approximately the same time as the corresponding peripheral inner-ring egg. In Experiment II, the core outer-ring egg had a higher incubation temperature than the inner-ring egg in the same set (e.g., 1.8°C in set 1). With a higher incubation temperature, the outer-ring egg may have developed more rapidly and eventually hatched earlier, producing the pattern described in Bi et al. (2021). Conversely, in the peripheral egg sets, the intra-ring temperature differences were small (e.g., 0.7°C in set 4). The outer-ring egg may have developed at an equal or only slightly faster rate than the inner-ring egg directly below it. Therefore, the inner-ring egg maintains the lead in the level of embryonic development and hatches earlier than the outer-ring egg immediately above it, resulting in the pattern described in Yang et al. (2019a). A similar case of temperature-induced hatching asynchrony has been observed in American Kestrels (*Falco* s*parverius*), which usually initiate incubation after the third or the fourth egg is laid in a clutch of four to five eggs (Bortolotti and Wiebe, 1993). Due to the kestrels' small body-to-clutch-volume ratio, their eggs are heated up unevenly and show hatching asynchrony (Bortolotti and Wiebe, 1993).

In a hotter environment such as that experienced by *Heyuannia* in the Nanxiong Group, the inner-ring eggs may have hatched earlier than their corresponding outer-ring eggs regardless of their proximity to the core. The average temperature differences between the outer and inner rings are minimal, ranging from -0.1°C to 0.4°C in Experiment III and 0.3°C to 1.0°C in both the posture and the non-posture simulations of Experiment III. With small differences in temperature, the outer- and inner-ring eggs may have similar developmental rates. Developing earlier, the inner-ring egg may have hatched earlier than the outer-ring egg of the same set, producing the pattern described in Yang et al. (2019a). Based on the experimental results, the less-developed inner-ring egg reported in Bi et al. (2021) could have been a case of failed embryonic development (Varricchio, 2021). An alternative explanation, considering the relative position between the outer- and inner-ring embryos compared in Bi et al. (2021), is that if the peripheral outer-ring egg were to be exposed to more solar heat, it might develop faster than a core inner-ring egg at a different position.

Considering that our interpretations of both intra-ring and inter-ring asynchronous hatching are based on the experimental design, three real-world scenarios could complicate the interpretations. Firstly, the arrangement of the eggs within the clutch with varying inclination angles, as seen in the original clutch and clutches discussed in Yang et al. (2019b), may alter the temperature distribution patterns. Secondly, a living and mobile adult, instead of an immobile one assumed in the experiments, might have produced different temperature distribution patterns. Still, even if the incubating adult was likely to move, we cannot completely exclude the possibility of inter- and intra-ring asynchronous hatching, as suggested by isotope-based temperature reconstructions and living examples of temperature-induced hatching asynchrony, despite the presence of only a single egg layer in the clutch (Bi et al., 2021; Bortolotti and Wiebe, 1993). Thirdly, the presence of the brooding adult's limbs within the clutch may have homogenized inter-ring temperature differences in smaller oviraptorid clutches (Hogan, 2024). As such, we concur with Hogan (2024) that hatching asynchrony may not have been ordered according to egg rings but instead subject to a complex temperature distribution pattern.

4.3.4 Thermoregulatory contact incubation and less efficient incubation in comparison to modern birds

To understand whether the thermodynamic advantage conferred by adult clutch attendance fulfills the criteria of TCI, the prerequisites are examined.

The first prerequisite of contacting all eggs is not fulfilled in our experimental model. In the generalized clutch, the outer ring prevents the incubator from contacting the inner ring. Since the eggs are partially buried and highly organized in the clutch, the brooding adult may not be able to manipulate the inner-ring eggs or contact them (Clark et al., 1999; Yang et al., 2019b). This result agrees with the inferences of Deeming (2002) and Yang et al. (2019b). Among the outer-ring eggs that are contacted, the greatest contact area is about 3% of the egg's total surface area (calculated from Wiemann et al., 2017). In contrast with the 8-10% contact area of chicken eggs (Ar et al., 2012), this proportion is relatively small and may be the cause of less efficient heat transfer and could be a factor in the longer incubation times expected in non-avian theropods (Varricchio et al., 2018).

The second prerequisite of the adult being the major heat source is fulfilled but with an incubation efficiency far lower than that of modern birds. The calculated incubation efficiency in Experiment II reaches at most 65%, well below the 84.3% reported for the common eider (*Somateria mollissima*) (Hogan and Varricchio, 2021). The low efficiency indicates that an oviraptorid may have partially relied on ambient heat sources to incubate the eggs in a clutch. With more reliance on solar heat than birds, an adult could still maintain eggs temperatures within the developmental ranges of crocodilian and avian embryos. In Experiment II, the equilibrium temperatures of the eggs ranged from 23.7°C to 30.2°C. This range overlaps with the field-observed 23.3°C to 32.8°C temperature range of *Alligator mississippiensis* eggs (Joanen, 1969). In Experiment III, nighttime minimum egg temperature was 30.4°C and daytime maximum temperature reached 37.4°C, consistent with the 30°C to 38°C incubation temperatures reported for Nanxiong oviraptorids (Amiot et al., 2017; Bi et al., 2021). The average 24-hour temperature, in the low 30s°C, also approximates the mean natural incubation temperature across a wide phylogeny of birds (Webb, 1987).

The third prerequisite of maintaining all eggs within a narrow range of temperature is not fulfilled by our experimental model. As discussed in *4.2.3*, the temperature differences within a clutch in Experiment II could result in intra- and inter-ring asynchronous hatching. While there are few intra- or inter-ring temperature differences in Experiment III, the diel fluctuations of eggs are

greater than those found in extant birds. Direct comparison of the temperature profile in Experiment III with that of wild ostrich eggs incubated in an environment with greater ambient temperature fluctuation shows that the experimental oviraptorid egg temperatures fluctuated by about 2°C more (Bertram and Burger, 1981). While it remains unknown how such temperature fluctuations might influence embryonic development, the wider range of egg temperatures indicates that the oviraptorid adult simulated in our experiments was less capable of regulating egg temperature to a similar extent to that of birds.

The prerequisites critical for TCI are not fulfilled. By induction, the results of this study do not support the hypothesis of oviraptorids conducting TCI. It is worth noting, nevertheless, that other interpretations of adult postures in the clutch, such as one in which the brooding adult places its legs in the egg-free center (Hogan, 2024), might have resulted in other patterns of contact between the brooding adult and the eggs and, accordingly, other temperature distribution patterns.

Instead of utilizing TCI, oviraptorids and the sun may be co-incubators. While an oviraptorid relies on the sun to raise the clutch temperature, the comparison between the attended and unattended clutch demonstrates that clutch attendance can maintain a substantially more stable microenvironment for embryonic development (Wang and Beissinger, 2011). The shade provided by the adult reduces the risk of embryonic hyperthermia. The heat conferred by the adult raises egg temperatures above the ambient temperature during nighttime. This comparatively less efficient incubation behavior, relative to modern birds, combines adult incubation and ambient heat sources, which could be a more ancestral state of incubation and the precursor of the TCI behavior.

4.3.5 Oviraptorid sex determination system

In extant animals, the development of offspring gonads can be determined by the sex chromosome or the accumulation of certain genetic products, a mechanism known as genotypic sex determination (GSD). Another type of sex-determining mechanism depends on the environmental conditions, such as temperature, social dynamics, or stress. It is known as environmental sex determination (ESD) (Weber and Capel, 2021). Among different types of ESD, crocodiles use temperature-dependent sex determination (TSD) (Deeming and Ferguson, 1991; Lang and Andrews, 1994), which is considered the ancestral state of Reptilia based on amino acid analysis (Janes et al., 2014). Birds, in contrast, use GSD. The initiation of avian testis development based on the dosage of the *dmrt1* gene on the Z chromosome is an apomorphy (Ioannidis et al., 2021). Previous studies suggest that the dinosaurs used the GSD system based on their low survivorship over the Cretaceous–Paleogene boundary compared to other TSD species (Deeming and Ferguson, 1991; Silber et al., 2011). Grellet-Tinner and Fiorelli (2010) also suggest that the neosauropods use the GSD system based on the constant incubation temperature maintained by the hydrothermal heat source. In contrast, Varricchio (2021) speculates that the temperature differences reported in Bi et al. (2021) indicate the use of the TSD system in oviraptorids. Here, we provide new insights into the sex-determination system of oviraptorids.

Extant TSD species incubate their eggs near the pivotal temperature, which is the temperature that yields 50% of offspring of each sex in a nest (Mrosovsky and Yntema, 1980), to avoid skewing the sex ratio of offspring (Ferrando-Bernal and Lao, 2022). Take crocodiles, for example, different species' pivotal temperatures range from 31.5°C to 31.8°C (for female-male transition) and 32.5°C to 34°C (for male-female transition) (Lang and Andrews, 1994). A field study documented that the eggs of the saltwater crocodile (*Crocodylus porosus*) are incubated in a cavity of 32.5 °C, which falls within the abovementioned pivotal temperature range (Magnusson, 1979). The pivotal temperature is relatively constant. It varies slightly both across different populations of loggerhead turtles (*Caretta caretta*) (less than 1°C; Mrosovsky, 1988) and related species (about 2.5°C across different genera of turtles compared by Mrosovsky, 1988; about 0.3°C among crocodiles compared in Lang and Andrews, 1994). Given that *Heyuannia* and *Nemegtomaia* are sister clades (Funston, 2020), it is parsimonious to assume that they share a similar pivotal temperature range if both species were to use TSD. However, in the experiments, the lower limit of *Heyuannia*'s incubation temperature (30.4°C) does not overlap with the upper limit of *Nemegtomaia's* (30.2°C). If the two species were to share a similar pivotal temperature range, most *Heyuannia* eggs would have been incubated above the presumed pivotal temperature, whereas most *Nemegtomaia* eggs below it, resulting in predominantly single-sex offspring for both species. In extant turtles and tuatara, deviation from the pivotal temperature tends to decrease hatching success in both male and female-biased populations (Grayson et al., 2014; Hays et al., 2017). The compounding influence of having sexually biased populations and reduced hatching success could greatly increase extirpation risk for the populations (Grayson et al., 2014).

Moreover, oviraptorids appeared to have occupied regions that are less favorable for TSD species. Extant TSD species tend to inhabit

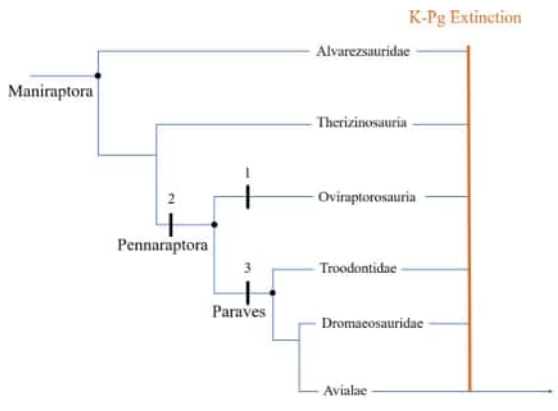

FIGURE 8
Simplified phylogeny showing hypothesized evolution of reproductive traits. Asynchronous hatching (number 1) could be a autapomorphy of Oviraptorosauria. Genotypic sex determination (number 2) could evolve in Pennaraptora or in even earlier lineages. While thermoregulatory contact incubation (number 3) could either evolve in Paraves or independently in Troodontidae and Avialae, the first inference is preferred here. The topology of the tree is based on Hendrickx et al. (2015) (Maniraptora) and Pei et al. (2020) (Paraves).

areas with significantly warmer ambient temperatures (mean 24.38° C), whereas GSD species with short breeding seasons (one to four months) inhabit areas with significantly colder ambient temperatures (Cornejo-Páramo et al., 2020). Given that the estimated maximum incubation period of the two oviraptorid species is less than four months (calculated from Deeming et al., 2006), the presence of *Nemegtomaia barsboldi* in an environment with a low warmest-month temperature is consistent with the biogeographic distribution of extant GSD species with short breeding season.

The hypothesis that oviraptorids utilized GSD is not contradicted by molecular clock analyses of avian ZW chromosomes. Although the recombination suppression of the ZW chromosomal segment appeared after the divergence between non-avian dinosaurs and Avialae species around 155 Ma (Nam and Ellegren, 2008; Wang and Lloyd, 2016), proto-sex chromosomes could take several millions of years or longer to accumulate enough mutations to become heterologous and thereby suppress recombination (Kratochvíl et al., 2021). Since the molecular clock cannot ascertain the precise timing of the ZW chromosome differentiation (Organ and Janes, 2008; Ellegren, 2013), oviraptorids could have used the GSD system.

4.3.6 Evolution of reproductive traits

Although uncertainty remains regarding the existence of multiple tiers in caenagnathid clutches, caenagnathids and oviraptorids may have had similar clutch configurations and potentially shared similar brooding behaviors (Tanaka et al., 2018a, *contra* Huh et al., 2014; Yang et al., 2019b). Our interpretation of oviraptorid reproductive biology, therefore, may apply to the clade Oviraptorosauria. If oviraptorosaurians used GSD, as birds do, the GSD system may have evolved in the common ancestor of oviraptorosaurians and birds, which could be Pennaraptora or even earlier lineages (Figure 8). While Grellet-Tinner and Fiorelli (2010) suggest that sauropods from Auca Mahuevo, Argentina, also use the GSD system, it is unknown if the GSD systems in theropods and sauropods have a shared evolutionary origin.

In contrast to most birds, which induce hatching asynchrony by incubating some eggs prior to the others in a nest, the temperature difference within an oviraptorosaurian clutch may have led to asynchronous embryonic developments, reaffirming Yang et al. (2019a)'s hypothesis of hatching asynchrony as a autapomorphy of oviraptorosaurians (Figure 8). Such an inference is also consistent with the understanding that troodontid eggs hatch synchronously and that hatching asynchrony has evolved independently in the avian lineage several times (Stoleson and Beissinger, 1995; Varricchio et al., 2002).

Regarding the evolution of the TCI behavior, the adult incubation efficiencies of *Troodon* (75.6%~83.1%) and birds (84.3%) are much higher than that of oviraptorids (26%~65%) (Hogan and Varricchio, 2021). It is likely that the TCI behavior evolved after the divergence of oviraptorosaurians from the lineage leading to troodontids and birds, possibly within Paraves. Nevertheless, the incubation efficiency and the embryonic hatching pattern of dromaeosaurids remain unknown despite the discoveries of an adult-associated egg of dromaeosaurid *Deinonychus antirrhopus* (Grellet-Tinner and Makovicky, 2006), a single-layered, center-devoid-of-egg dromaeosaurid clutch in North America (Zelenitsky and Therrien, 2008), and a likely small dromaeosaurid clutch in Japan (Tanaka et al., 2020). The TCI behavior could as well have evolved independently in troodontids and birds.

4.4 Potentials for future investigations

With the current state of knowledge, it remains unclear whether dromaeosaurids conducted TCI. The discovery of more complete adult-associated dromaeosaurid clutches would help cast light on the evolution of TCI behavior.

While the model tested in this study provides a general explanation for asynchronous hatching patterns in oviraptorosaurians, real temperature distributions may be complicated by parental behavior, thermogenesis of the embryo, and daily temperature fluctuations (Whittow and Tazawa, 1991; Georges et al., 2005). For example, avian egg incubation temperature can vary "substantially" during different stages of development (Webb, 1987), with late-stage embryos having higher average temperatures (Booth, 1987; Boulton and Cassey, 2012).

Future models examining how incubation temperature influences crocodilian and avian embryonic development rates at different development stages are needed to phylogenetically bracket and estimate the development of oviraptorosaurian embryos under varying incubation temperatures. A study of the pig-nosed turtle (*Carettochelys insculpta*) modeled developmental progress using changes in head width (Georges et al., 2005). Similar approaches, combined with additional analyses such as cranial morphology comparisons, may help assess the incubation periods of embryo fossils (Chapelle et al., 2020).

5 Conclusion

This study reconstructs realistic oviraptorid clutches and employs numerical simulations to investigate the heat transfer in an adult-associated clutch. Our results show that the oviraptorosaurian adult, modeled on *Heyuannia huangi*, contacts none of the inner-ring eggs in the reconstructed clutch, relies partially on environmental heat sources for incubation, and induces temperature variation within the clutch through its posture. These findings do not support the hypothesis that oviraptorosaurians utilized thermoregulatory contact incubation in the manner of extant birds. Instead, the brooding adult transferred heat less efficiently to the eggs and co-regulated egg temperature in conjunction with solar input.

We also find evidence consistent with asynchronous hatching in oviraptorosaurian embryos. In a *Nemegtomaia* clutch, the core outer-ring egg would hatch earlier than the inner-ring egg immediately beneath it, whereas the peripheral inner-ring egg would hatch earlier than the corresponding outer-ring egg. In a *Heyuannia* clutch, inner-ring eggs would hatch earlier regardless of position. Interpreting hatching asynchrony as posture-induced not

only reconciles contrasting hatching patterns found in the fossil record but also supports the inference that hatching asynchrony is a shared derived trait within Oviraptorosauria.

Furthermore, the substantial difference in incubation temperature ranges between *Nemegtomaia* and *Heyuannia* suggests that oviraptorosaurians likely did not have temperature-dependent sex determination. If they had TSD, the large temperature differences we recovered could have produced skewed sex ratios. Overall, the methods and findings of this study demonstrate a strong potential for quantitative thermal experimentation and modeling as a means to investigate the behavioral and reproductive biology of extinct animals that have no extant analog.

Data availability statement

The original contributions presented in the study are included in the article/Supplementary Material. Further inquiries can be directed to the corresponding authors.

Author contributions

CS: Conceptualization, Data curation, Formal analysis, Investigation, Methodology, Software, Supervision, Validation, Visualization, Writing – original draft, Writing – review & editing. JL: Methodology, Software, Writing – review & editing. HW: Data curation, Methodology, Software, Visualization, Writing – review & editing. KC: Data curation, Methodology, Software, Writing – review & editing. CC: Data curation, Methodology, Software, Visualization, Writing – review & editing. ML: Data curation, Methodology, Software, Writing – review & editing, Conceptualization, Resources, Supervision, Validation. TY: Conceptualization, Data curation, Methodology, Resources, Software, Supervision, Validation, Writing – review & editing, Formal analysis, Funding acquisition, Investigation, Project administration, Visualization, Writing – original draft.

Funding

The author(s) declared that financial support was received for this work and/or its publication. This study is supported by the research grant of the National Science and Technology Council (No. 111-2116-M178-004- and 113-2116-M-178-001), Taiwan, to TY.

Acknowledgments

The authors would like to thank NMNS for access to the collection of oviraptorid clutch specimens and skeleton display. CS would like to thank Bo-Wei Chen for his relentless and invaluable guidance, Kun-Ming Chuang for instructing the use of molding equipment, Chun-Chi Su and Hui-Ling Chen for facility space for experimentation, and Yun-Ju Chen, Shi-Xian Lien, Yu-Tsung Tai, Sin-Bo Guan, and Ching-Hsien Cheng for their support.

Conflict of interest

The authors declared that this work was conducted in the absence of any commercial or financial relationships that could be construed as a potential conflict of interest.

Generative AI statement

The author(s) declared that generative AI was not used in the creation of this manuscript.

Any alternative text (alt text) provided alongside figures in this article has been generated by Frontiers with the support of artificial intelligence and reasonable efforts have been made to ensure accuracy, including review by the authors wherever possible. If you identify any issues, please contact us.

Publisher's note

Supplementary material

The Supplementary Material for this article can be found online at: https://www.frontiersin.org/articles/10.3389/fevo.2026.1351288/full#supplementary-material

References

Abbasnezhad, B., Hamdami, N., Monteau, J. Y., and Vatankhah, H. (2016). Numerical modeling of heat transfer and pasteurizing value during thermal processing of intact egg. *Food Sci. Nutr.* 4, 42–49. doi: 10.1002/fsn3.257

Amiot, R., Lécuyer, C., Buffetaut, E., Escarguel, G., Fluteau, F., and Martineau, F. (2006). Oxygen isotopes from biogenic apatites suggest widespread endothermy in Cretaceous dinosaurs. *Earth Planet. Sci. Lett.* 246, 41–54. doi: 10.1016/j.epsl.2006.04.018

Amiot, R., Wang, X., Wang, S., Lécuyer, C., Mazin, J. M., Mo, J., et al. (2017). $\delta^{18}O$-derived incubation temperatures of oviraptorosaur eggs. *Palaeontology* 60, 633–647. doi: 10.1111/pala.12311

Ar, A., Posmanik, R., Shmueli-Bauer, I., and Rozenboim, I. (2012). "The dynamic role of the brood patch as part of the microclimate of the egg in the nest," in Abstracts: Nest construction and function. *Avian Biol. Res.* 6, 183-185. doi: 10.3184/175815513X13615531066791

Berdahl, P., and Fromberg, R. (1982). The thermal radiance of clear skies. *Solar Energy* 29, 299–314. doi: 10.1016/0038-092X(82)90245-6

Bertram, B. C. (1992). *The ostrich communal nesting system* (Princeton: Princeton University Press).

Bertram, B., and Burger, A. (1981). Aspects of incubation in ostriches. *Ostrich* 52, 36–43. doi: 10.1080/00306525.1981.9633581

Bi, S., Amiot, R., de Fabrègues, C. P., Pittman, M., Lamanna, M. C., Yu, Y., et al. (2021). An oviraptorid preserved atop an embryo-bearing egg clutch sheds light on the reproductive biology of non-avialan theropod dinosaurs. *Sci. Bull.* 66, 947–954. doi: 10.1016/j.scib.2020.12.018

Booth, D. T. (1987). Effect of temperature on development of mallee fowl Leipoa ocellata eggs. *Physiol. Zool.* 60, 437–445. doi: 10.1086/physzool.60.4.30157905

Bortolotti, G. R., and Wiebe, K. L. (1993). Incubation behaviour and hatching patterns in the American kestrel *Falco sparverius*. *Ornis Scandinav.* 1, 41–47. doi: 10.2307/3676408

Boulton, R. L., and Cassey, P. (2012). How avian incubation behaviour influences egg surface temperatures: relationships with egg position, development and clutch size. *J. Avian Biol.* 43, 289–296. doi: 10.1111/j.1600-048X.2012.05657.x

Bourke, J. M. (2015). *Implications of airflow dynamics and soft-tissue reconstructions for the heat exchange potential of dinosaur nasal passages*. [dissertation]. [Athens (OH)]: Ohio University.

Buttemer, W. A., Astheimer, L. B., and Dawson, T. J. (1988). Thermal and water relations of emu eggs during natural incubation. *Physiol. Zool.* 61, 483–494. doi: 10.1086/physzool.61.6.30156156

Campione, N. E., and Evans, D. C. (2012). A universal scaling relationship between body mass and proximal limb bone dimensions in quadrupedal terrestrial tetrapods. *BMC Biol.* 10, 1–22. doi: 10.1186/1741-7007-10-60

Carter, T. (1968). The hen's egg: density of egg shell and egg contents. *Br. Poultry Sci.* 9, 265–271. doi: 10.1080/00071666808415718

Chapelle, K. E., Fernandez, V., and Choiniere, J. N. (2020). Conserved in-ovo cranial ossification sequences of extant saurians allow estimation of embryonic dinosaur developmental stages. *Sci. Rep.* 10, 1–10. doi: 10.1038/s41598-020-60292-z

Cheng, Y. N., Qiang, J., Wu, X. C., and Shan, H. Y. (2008). Oviraptorosaurian eggs (Dinosauria) with embryonic skeletons discovered for the first time in China. *Acta Geol. Sinica-English Edition* 82, 1089–1094. doi: 10.1111/j.1755-6724.2008.tb00708.x

Chiappe, L. M., Schmitt, J. G., Jackson, F. D., Garrido, A., Dingus, L., and Grellet-Tinner, G. (2004). Nest structure for sauropods: sedimentary criteria for recognition of dinosaur nesting traces. *Palaios* 19, 89–95. doi: 10.1669/0883-1351(2004)019<0089:NSFSSC>2.0.CO;2

Christiansen, P. (1999a). Long bone scaling and limb posture in non-avian theropods: evidence for differential allometry. *J. Vertebrate Paleontol.* 19, 666–680. doi: 10.1080/02724634.1999.10011180

Christiansen, P. (1999b). Scaling of the limb long bones to body mass in terrestrial mammals. *J. Morphol.* 239, 167–190. doi: 10.1002/(SICI)1097-4687(199902)239:2<167::AID-JMOR5>3.0.CO;2-8

Clark, J. M., Norell, M., Chiappe, L. M., Akademi, M. S. U., and Project, M.-A. M. P. (1999). An oviraptorid skeleton from the late Cretaceous of Ukhaa Tolgod, Mongolia, preserved in an avianlike brooding position over an oviraptorid nest. *Am. Museum Novitates* 3265, 1-35. doi: 10.1206/0003-0082(1999)265<0001:AOSFTL>2.0.CO;2

Conway, C. J., and Martin, T. E. (2000). Effects of ambient temperature on avian incubation behavior. *Behav. Ecol.* 11, 178–188. doi: 10.1093/beheco/11.2.178

Cornejo-Páramo, P., Lira-Noriega, A., Ramírez-Suástegui, C., Méndez-De-La-Cruz, F. R., Székely, T., Urrutia, A. O., et al. (2020). Sex determination systems in reptiles are related to ambient temperature but not to the level of climatic fluctuation. *BMC Evol. Biol.* 20, 1–14. doi: 10.1186/s12862-020-01671-y

Deeming, D. C. (2002). *Avian incubation: behaviour, environment and evolution* (Oxford: Oxford University Press).

Deeming, D. C. (2006). Ultrastructural and functional morphology of eggshells supports the idea that dinosaur eggs were incubated buried in a substrate. *Palaeontology* 49, 171–185. doi: 10.1111/j.1475-4983.2005.00536.x

Deeming, D. C., Birchard, G., Crafer, R., and Eady, P. (2006). Egg mass and incubation period allometry in birds and reptiles: effects of phylogeny. *J. Zool.* 270, 209–218. doi: 10.1111/j.1469-7998.2006.00131.x

Deeming, D. C., and Ferguson, M. W. (1991). *Egg incubation: its effects on embryonic development in birds and reptiles* (Cambridge: Cambridge University Press).

Dekker, R. W. (2007). "Distribution and speciation of megapodes (Megapodiidae) and subsequent development of their breeding," in *Biogeography, time, and place: distributions, barriers, and islands* (Dordrecht: Springer), 93–102.

Denys, S., Pieters, J., and Dewettinck, K. (2003). Combined CFD and experimental approach for determination of the surface heat transfer coefficient during thermal processing of eggs. *J. Food Sci.* 68, 943–951. doi: 10.1111/j.1365-2621.2003.tb08269.x

Dong, Z.-M., and Currie, P. J. (1996). On the discovery of an oviraptorid skeleton on a nest of eggs at Bayan Mandahu, Inner Mongolia, People's Republic of China. *Can. J. Earth Sci.* 33, 631–636. doi: 10.1139/e96-046

Downs, C. T., and Ward, D. (1997). Does shading behavior of incubating shorebirds in hot environments cool the eggs or the adults? *Auk* 114, 717–724. doi: 10.2307/4089291

Eagle, R. A., Enriquez, M., Grellet-Tinner, G., Pérez-Huerta, A., Hu, D., Tütken, T., et al. (2015). Isotopic ordering in eggshells reflects body temperatures and suggests differing thermophysiology in two Cretaceous dinosaurs. *Nat. Commun.* 6, 8296. doi: 10.1038/ncomms9296

Ellegren, H. (2013). The evolutionary genomics of birds. *Annu. Rev. Ecol. Evol. Syst.* 44, 239–259. doi: 10.1146/annurev-ecolsys-110411-160327

Fanti, F., Currie, P. J., and Badamgarav, D. (2012). New specimens of nemegtomaia from the baruungoyot and nemegt formations (Late cretaceous) of Mongolia. *PloS One* 7, e31330. doi: 10.1371/journal.pone.0031330

Farlow, J. O., Thompson, C. V., and Rosner, D. E. (1976). Plates of the dinosaur Stegosaurus: forced convection heat loss fins? *Science* 192, 1123–1125. doi: 10.1126/science.192.4244.1123

Ferrando-Bernal, M., and Lao, O. (2022). Genotypic sex determination systems could be adaptations to extreme temperature environments in reptiles and to endothermy in mammals and birds. *bioRxiv*. doi: 10.1101/2022.02.07.479281

Foth, C., Tischlinger, H., and Rauhut, O. W. (2014). New specimen of Archaeopteryx provides insights into the evolution of pennaceous feathers. *Nature* 511, 79–82. doi: 10.1038/nature13467

Funston, G. (2020). Caenagnathids of the Dinosaur Park Formation (Campanian) of Alberta, Canada: anatomy, osteohistology, taxonomy, and evolution. *Vertebrate Anat. Morphol. Palaeontol.* 8, 105–153. doi: 10.18435/vamp29362

Georges, A., Beggs, K., Young, J. E., and Doody, J. S. (2005). Modelling development of reptile embryos under fluctuating temperature regimes. *Physiol. Biochem. Zool.* 78, 18–30. doi: 10.1086/425200

Georges, A., Limpus, C., and Stoutjesdijk, R. (1994). Hatchling sex in the marine turtle Caretta caretta is determined by proportion of development at a temperature, not daily duration of exposure. *J. Exp. Zool.* 270, 432–444. doi: 10.1002/jez.1402700504

Gliah, O., Kruczek, B., Etemad, S. G., and Thibault, J. (2011). The effective sky temperature: an enigmatic concept. *Heat Mass Transfer* 47, 1171–1180. doi: 10.1007/s00231-011-0780-1

Grayson, K. L., Mitchell, N. J., Monks, J. M., Keall, S. N., Wilson, J. N., and Nelson, N. J. (2014). Sex ratio bias and extinction risk in an isolated population of tuatara (*Sphenodon punctatus*). *PloS One* 9, e94214. doi: 10.1371/journal.pone.0094214

Grellet-Tinner, G., and Fiorelli, L. E. (2010). A new Argentinean nesting site showing neosauropod dinosaur reproduction in a Cretaceous hydrothermal environment. *Nat. Commun.* 1, 1–8. doi: 10.1038/ncomms1031

Grellet-Tinner, G., and Makovicky, P. (2006). A possible egg of the dromaeosaur *Deinonychus antirrhopus*: phylogenetic and biological implications. *Can. J. Earth Sci.* 43, 705–719. doi: 10.1139/e06-033

Grenier, J. L., and Beissinger, S. R. (1999). Variation in the onset of incubation in a neotropical parrot. *Condor* 101, 752–761. doi: 10.2307/1370062

Griffith, S. C., Mainwaring, M. C., Sorato, E., and Beckmann, C. (2016). High atmospheric temperatures and 'ambient incubation'drive embryonic development and lead to earlier hatching in a passerine bird. *R. Soc. Open Sci.* 3, 150371. doi: 10.1098/rsos.150371

Hartman, S. (2003). *Skeletal Drawing Heyuannia huangi*. Available online at: https://www.skeletaldrawing.com/theropods/heyuannia (Accessed August 24, 2023).

Hartman, S. A., Lovelace, D. M., Linzmeier, B. J., Mathewson, P. D., and Porter, W. P. (2022). Mechanistic thermal modeling of late triassic terrestrial amniotes predicts biogeographic distribution. *Diversity* 14, 973. doi: 10.3390/d14110973

Hassan, S., Siam, A., Mady, M., and Cartwright, A. (2004). Incubation temperature for ostrich (*Struthio camelus*) eggs. *Poultry Sci.* 83, 495–499. doi: 10.1093/ps/83.3.495

Hays, G. C., Mazaris, A. D., Schofield, G., and Laloë, J.-O. (2017). Population viability at extreme sex-ratio skews produced by temperature-dependent sex determination. *Proc. R. Soc. B: Biol. Sci.* 284, 20162576. doi: 10.1098/rspb.2016.2576

Hendrickx, C., Hartman, S. A., and Mateus, O. (2015). An overview of non-avian theropod discoveries and classification. *PalArch's J. Vertebrate Palaeontol.* 12, 1–73. doi: 10.35535/palaeo.13.2.1

Hepp, G. R., Kennamer, R. A., and Johnson, M. H. (2006). Maternal effects in Wood Ducks: incubation temperature influences incubation period and neonate phenotype. *Funct. Ecol.* 20, 307–314. doi: 10.1111/j.1365-2435.2006.01108.x

Hogan, J. D., and Varricchio, D. J. (2021). Do paleontologists dream of electric dinosaurs? Investigating the presumed inefficiency of dinosaurs contact incubating partially buried eggs. *Paleobiology* 47, 101–114. doi: 10.1017/pab.2020.49

Hogan, J. D. (2024). The egg-thief architect: experimental oviraptorosaur nesting physiology, the possibility of adult-mediated incubation, and the feasibility of indirect contact incubation. *Paleobiology* 50, 108–102.

Hopp, T. P., and Orsen, M. J. (2004). "11. Dinosaur brooding behavior and the origin of flight feathers," in *Feathered dragons: studies on the transition from dinosaurs to birds*. Eds. P. J. Currie, E. B. Koppelhus, M. A. Shugar and J. L. Wright (Indiana University Press, Bloomington), 234–250.

Hoyt, D. F., Vleck, D., and Vleck, C. M. (1978). Metabolism of avian embryos: ontogeny and temperature effects in the ostrich. *Condor* 80, 265–271. doi: 10.2307/1368034

Huh, M., Kim, B. S., Woo, Y., Simon, D. J., Paik, I. S., and Kim, H. J. (2014). First record of a complete giant theropod egg clutch from Upper Cretaceous deposits, South Korea. *Historical Biol.* 26, 218–228. doi: 10.1080/08912963.2014.894998

Hutton, J. (1987). Incubation temperatures, sex ratios and sex determination in a population of Nile crocodiles (*Crocodylus niloticus*). *J. Zool.* 211, 143–155. doi: 10.1111/j.1469-7998.1987.tb07458.x

Incropera, F. P., DeWitt, D. P., Bergman, T. L., and Lavine, A. S. (2006). *Fundamentals of heat and mass transfer. 6th ed* Vol. 6 (New York: Wiley).

Ioannidis, J., Taylor, G., Zhao, D., Liu, L., Idoko-Akoh, A., Gong, D., et al. (2021). Primary sex determination in birds depends on DMRT1 dosage, but gonadal sex does not determine adult secondary sex characteristics. *Proc. Natl. Acad. Sci.* 118. doi: 10.1073/pnas.2020909118

Jackson, F. D., Varricchio, D. J., Jackson, R. A., Vila, B., and Chiappe, L. M. (2008). Comparison of water vapor conductance in a titanosaur egg from the Upper Cretaceous of Argentina and a *Megaloolithus siruguei* egg from Spain. *Paleobiology* 34, 229–246. doi: 10.1666/0094-8373(2008)034[0229:COWVCI]2.0.CO;2

Janes, D. E., Organ, C. L., Stiglec, R., O'Meally, D., Sarre, S. D., Georges, A., et al. (2014). Molecular evolution of Dmrt1 accompanies change of sex-determining mechanisms in reptilia. *Biol. Lett.* 10, 20140809. doi: 10.1098/rsbl.2014.0809

Jin, X., Varricchio, D. J., Poust, A. W., and He, T. (2019). An oviraptorosaur adult-egg association from the Cretaceous of Jiangxi Province, China. *J. Vertebrate Paleontol.* 39, e1739060. doi: 10.1080/02724634.2019.1739060

Joanen, T. (1969). Nesting ecology of alligators in Louisiana. *J. Southeastern Assoc. Fish Wildlife Agencies* 23, 141–151.

Kratochvíl, L., Stöck, M., Rovatsos, M., Bullejos, M., Herpin, A., Jeffries, D. L., et al. (2021). Expanding the classical paradigm: what we have learnt from vertebrates about sex chromosome evolution. *Philos. Trans. R. Soc. B* 376, 20200097. doi: 10.1098/rstb.2020.0097

Ksepka, D. T. (2020). Feathered dinosaurs. *Curr. Biol.* 30, R1347–R1353. doi: 10.1016/j.cub.2020.10.007

Kumar, S., and Mullick, S. (2010). Wind heat transfer coefficient in solar collectors in outdoor conditions. *Solar Energy* 84, 956—963. doi: 10.1016/j.solener.2010.03.003

Lang, J. W., and Andrews, H. V. (1994). Temperature-dependent sex determination in crocodilians. *J. Exp. Zool.* 270, 28–44. doi: 10.1002/jez.1402700105

Lü, J. (2003). A new oviraptorosaurid (Theropoda: Oviraptorosauria) from the Late Cretaceous of southern China. *J. Vertebrate Paleontol.* 22, 871–875. doi: 10.1671/0272-4634(2002)022[0871:ANOTOF]2.0.CO;2

Lundy, H. (1969). "A review of the effects of temperature, humidity, turning and gaseous environment in the incubator on the hatchability of the hen's egg," in *The fertility and hatchability of hen's egg*. Oliver and Boyd at Edinburg.

Ma, M., Liu, X., and Wang, W. (2018). Palaeoclimate evolution across the Cretaceous–Palaeogene boundary in the Nanxiong Basin (SE China) recorded by red strata and its correlation with marine records. *Climate Past* 14, 287–302. doi: 10.5194/cp-14-287-2018

Magnusson, W. E. (1979). Maintenance of temperature of crocodile nests (Reptilia, Crocodilidae). *J. Herpetol.*, 439–443. doi: 10.2307/1563479

McQuillan, F., Culham, J., and Yovanovich, M. (1984). Properties of dry air as one atmosphere, microelectronics heat transfer lab. *Rept. UW/M HTL 8406*.

Mira, M., Valor, E., Boluda, R., Caselles, V., and Coll, C. (2007). Influence of soil water content on the thermal infrared emissivity of bare soils: Implication for land surface temperature determination. *J. Geophys. Res.: Earth Surface* 112. doi: 10.1029/2007JF000749

Mrosovsky, N. (1988). Pivotal temperatures for loggerhead turtles (*Caretta caretta*) from northern and southern nesting beaches. *Can. J. Zool.* 66, 661–669. doi: 10.1139/z88-098

Mrosovsky, N., and Yntema, C. (1980). Temperature dependence of sexual differentiation in sea turtles: implications for conservation practices. *Biol. Conserv.* 18, 271–280. doi: 10.1016/0006-3207(80)90003-8

Nam, K., and Ellegren, H. (2008). The chicken (*Gallus gallus*) Z chromosome contains at least three nonlinear evolutionary strata. *Genetics* 180, 1131–1136. doi: 10.1534/genetics.108.090324

Norell, M. A., Balanoff, A. M., Barta, D. E., and Erickson, G. M. (2018). A second specimen of *Citipati Osmolskae* associated with a nest of eggs from Ukhaa Tolgod, Omnogov Aimag, Mongolia. *Am. Museum Novitates* 2018, 1–44, 44. doi: 10.5962/bhl.title.156722

Norell, M. A., Clark, J. M., and Chiappe, L. M. (2001). An embryonic oviraptorid (Dinosauria: Theropoda) from the upper Cretaceous of Mongolia. *Am. Museum Novitates* 2001, 1–20. doi: 10.1206/0003-0082(2001)315<0001:AEODTF>2.0.CO;2

Norell, M. A., Clark, J. M., Chiappe, L. M., and Dashzeveg, D. (1995). A nesting dinosaur. *Nature* 378, 774–776. doi: 10.1038/378774a0

O'Connor, M. P., and Dodson, P. (1999). Biophysical constraints on the thermal ecology of dinosaurs. *Paleobiology* 25, 341–368. doi: 10.1017/S0094837300021321

Organ, C. L., and Janes, D. E. (2008). Evolution of sex chromosomes in Sauropsida. *Integr. Comp. Biol.* 48, 512–519. doi: 10.1093/icb/icn041

Organ, C. L., Shedlock, A. M., Meade, A., Pagel, M., and Edwards, S. V. (2007). Origin of avian genome size and structure in non-avian dinosaurs. *Nature* 446, 180–184. doi: 10.1038/nature05621

Osborn, H. F., Kaisen, P. C., and Olsen, G. (1924). Three new theropoda, *Protoceratops* zone, central Mongolia. *Am. Museum Novitates*, no. 144, 1-12.

Owocki, K., Kremer, B., Cotte, M., and Bocherens, H. (2020). Diet preferences and climate inferred from oxygen and carbon isotopes of tooth enamel of *Tarbosaurus bataar* (Nemegt Formation, Upper Cretaceous, Mongolia). *Palaeogeogr. Palaeoclimatol. Palaeoecol.* 537, 109190. doi: 10.1016/j.palaeo.2019.05.012

Parker, S. L., and Andrews, R. M. (2007). Incubation temperature and phenotypic traits of *Sceloporus undulatus*: implications for the northern limits of distribution. *Oecologia* 151, 218–231. doi: 10.1007/s00442-006-0583-0

Pei, R., Pittman, M., Goloboff, P. A., Dececchi, T. A., Habib, M. B., Kaye, T. G., et al. (2020). Potential for powered flight neared by most close avialan relatives, but few crossed its thresholds. *Curr. Biol.* 30, 4033–4046.e4038. doi: 10.1016/j.cub.2020.06.105

Reisz, R. R., Evans, D. C., Roberts, E. M., Sues, H.-D., and Yates, A. M. (2012). Oldest known dinosaurian nesting site and reproductive biology of the Early Jurassic sauropodomorph *Massospondylus*. *Proc. Natl. Acad. Sci.* 109, 2428–2433. doi: 10.1073/pnas.1109385109

Robin, P., Cellier, P., and Richard, G. (1997). Theoretical and field comparison of two types of soil heat fluxmeter. *Soil Technol.* 10, 185–206. doi: 10.1016/S0933-3630(96)00125-0

Ruxton, G. D., Birchard, G. F., and Deeming, D. C. (2014). Incubation time as an important influence on egg production and distribution into clutches for sauropod dinosaurs. *Paleobiology* 40, 323–330. doi: 10.1666/13028

Sabliov, C. M., Farkas, B. E., Keener, K. M., and Curtis, P. A. (2002). Cooling of shell eggs with cryogenic carbon dioxide: a finite element analysis of heat transfer. *LWT-Food Sci. Technol.* 35, 568–574. doi: 10.1016/S0023-6438(02)90915-1

Sato, T., Cheng, Y. N., Wu, X. C., Zelenitsky, D. K., and Hsiao, Y. F. (2005). A pair of shelled eggs inside a female dinosaur. *Science* 308, 375. doi: 10.1126/science.1110578

Seebacher, F. (2001). A new method to calculate allometric length-mass relationships of dinosaurs. *J. Vertebrate Paleontol.* 21, 51–60. doi: 10.1671/0272-4634(2001)021[0051:ANMTCA]2.0.CO;2

Seymour, R. S. (1979). Dinosaur eggs: gas conductance through the shell, water loss during incubation and clutch size. *Paleobiology* 5, 1–11. doi: 10.1017/S0094837300006242

Silber, S., Geisler, J. H., and Bolortsetseg, M. (2011). Unexpected resilience of species with temperature-dependent sex determination at the Cretaceous–Palaeogene boundary. *Biol. Lett.* 7, 295–298. doi: 10.1098/rsbl.2010.0882

Stoleson, S. H., and Beissinger, S. R. (1995). "Hatching asynchrony and the onset of incubation in birds, revisited," in *Current ornithology* (Springer), 191–270.

Tanaka, K., Zelenitsky, D. K., Lü, J., DeBuhr, C. L., Yi, L., Jia, S., et al. (2018a). Incubation behaviours of oviraptorosaur dinosaurs in relation to body size. *Biol. Lett.* 14, 20180135. doi: 10.1098/rsbl.2018.0135

Tanaka, K., Zelenitsky, D. K., and Therrien, F. (2015). Eggshell porosity provides insight on evolution of nesting in dinosaurs. *PloS One* 10, e0142829. doi: 10.1371/journal.pone.0142829

Tanaka, K., Zelenitsky, D. K., Therrien, F., Ikeda, T., Kubota, K., Saegusa, H., et al. (2020). Exceptionally small theropod eggs from the Lower Cretaceous Ohyamashimo Formation of Tamba, Hyogo Prefecture, Japan. *Cretaceous Res.* 114, 104519. doi: 10.1016/j.cretres.2020.104519

Tanaka, K., Zelenitsky, D. K., Therrien, F., and Kobayashi, Y. (2018b). Nest substrate reflects incubation style in extant archosaurs with implications for dinosaur nesting habits. *Sci. Rep.* 8, 1–10. doi: 10.1038/s41598-018-21386-x

Tarnawski, V. R., Momose, T., Leong, W. H., and Piper, D. J. W. (2011). "Estimation of quartz content in mineral soils," in *Encyclopedia of agrophysics*. Eds. J. Gliński, J. Horabik and J. Lipiec (Springer Netherlands, Dordrecht), 275–280.

Turner, J. (2002). Maintenance of egg temperature. *Oxford Ornithol. Ser.* 13, 119–142. doi: 10.1093/oso/9780198508106.003.0009

Varricchio, D. J. (2021). An exceptional adult-clutch-embryo association and its implications for dinosaur reproduction. *Sci. Bull.* 66, 868–870. doi: 10.1016/j.scib.2021.02.015

Varricchio, D. J., Horner, J. R., and Jackson, F. D. (2002). Embryos and eggs for the Cretaceous theropod dinosaur *Troodon formosus*. *J. Vertebrate Paleontol.* 22, 564–576. doi: 10.1671/0272-4634(2002)022[0564:EAEFTC]2.0.CO;2

Varricchio, D. J., Jackson, F., Borkowski, J. J., and Horner, J. R. (1997). Nest and egg clutches of the dinosaur *Troodon formosus* and the evolution of avian reproductive traits. *Nature* 385, 247–250. doi: 10.1038/385247a0

Varricchio, D. J., Jackson, F. D., Jackson, R. A., and Zelenitsky, D. K. (2013). Porosity and water vapor conductance of two *Troodon formosus* eggs: an assessment of incubation strategy in a maniraptoran dinosaur. *Paleobiology* 39, 278–296. doi: 10.1666/11042

Varricchio, D. J., Jackson, F., and Trueman, C. N. (1999). A nesting trace with eggs for the Cretaceous theropod dinosaur *Troodon formosus*. *J. Vertebrate Paleontol.* 19, 91–100. doi: 10.1080/02724634.1999.10011125

Varricchio, D. J., Kundrát, M., and Hogan, J. (2018). An intermediate incubation period and primitive brooding in a theropod dinosaur. *Sci. Rep.* 8, 1–6. doi: 10.1038/s41598-018-30085-6

Veghte, J. H., and Herreid, C. F. (1965). Radiometric determination of feather insulation and metabolism of arctic birds. *Physiol. Zool.* 38, 267–275. doi: 10.1086/physzool.38.3.30152838

Wagner, T. L., Wu, H.-I., Sharpe, P. J., Schoolfield, R. M., and Coulson, R. N. (1984). Modeling insect development rates: a literature review and application of a biophysical model. *Ann. Entomol. Soc. America* 77, 208–220. doi: 10.1093/aesa/77.2.208

Wang, J. M., and Beissinger, S. R. (2011). Partial incubation in birds: its occurrence, function, and quantification. *Auk* 128, 454–466. doi: 10.1525/auk.2011.10208

Wang, M., and Lloyd, G. T. (2016). Rates of morphological evolution are heterogeneous in Early Cretaceous birds. *Proc. R. Soc. B: Biol. Sci.* 283, 20160214. doi: 10.1098/rspb.2016.0214

Webb, D. (1987). Thermal tolerance of avian embryos: a review. *Condor* 89, 874–898. doi: 10.2307/1368537

Weber, C., and Capel, B. (2021). Sex determination without sex chromosomes. *Philos. Trans. R. Soc. B* 376, 20200109. doi: 10.1098/rstb.2020.0109

Weiß, R. (2020). *Reproductive biology of Oviraptorosauria: Evidence from a historic eggshell collection from the Late Cretaceous Nanxiong Basin, South China* (Rheinische Friedrich-Wilhelms-Universität Bonn).

Weishampel, D. B., Fastovsky, D. E., Watabe, M., Varricchio, D., Jackson, F., Tsogtbaatar, K., et al. (2008). New oviraptorid embryos from Bugin-Tsav, Nemegt Formation (Upper Cretaceous), Mongolia, with insights into their habitat and growth. *J. Vertebrate Paleontol.* 28, 1110–1119. doi: 10.1671/0272-4634-28.4.1110

Whittow, G. C., and Tazawa, H. (1991). The early development of thermoregulation in birds. *Physiol. Zool.* 64, 1371–1390. doi: 10.1086/physzool.64.6.30158220

Wiemann, J., Yang, T.-R., and Norell, M. A. (2018). Dinosaur egg colour had a single evolutionary origin. *Nature* 563, 555–558. doi: 10.1038/s41586-018-0646-5

Wiemann, J., Yang, T.-R., Sander, P. N., Schneider, M., Engeser, M., Kath-Schorr, S., et al. (2017). Dinosaur origin of egg color: oviraptors laid blue-green eggs. *PeerJ* 5, e3706. doi: 10.7717/peerj.3706

Xing, L., Niu, K., Ma, W., Zelenitsky, D. K., Yang, T.-R., and Brusatte, S. L. (2021). An exquisitely preserved in-ovo theropod dinosaur embryo sheds light on avian-like prehatching postures. *iScience* 25, 103516. doi: 10.1016/j.isci.2021.103516

Yang, T.-R. (2012). *Brooding behaviors of Late Cretaceous oviraptoroid dinosaurs from China* (Tainan, Taiwan: National Cheng Kung University).

Yang, T.-R., Chen, Y.-H., Wiemann, J., Spiering, B., and Sander, P. M. (2018). Fossil eggshell cuticle elucidates dinosaur nesting ecology. *PeerJ* 6, e5144. doi: 10.7717/peerj.5144

Yang, T.-R., Engler, T., Lallensack, J. N., Samathi, A., Makowska, M., and Schillinger, B. (2019a). Hatching asynchrony in oviraptorid dinosaurs sheds light on their unique nesting biology. *Integr. Organismal Biol.* 1, obz030. doi: 10.1093/iob/obz030

Yang, K., Koike, T., Ye, B., and Bastidas, L. (2005). Inverse analysis of the role of soil vertical heterogeneity in controlling surface soil state and energy partition. *J. Geophys. Res.: Atmospheres* 110, D08181. doi: 10.1029/2004JD005500

Yang, T.-R., and Sander, P. M. (2022). *The reproductive biology of oviraptorosaurs: a synthetic view* (London: Geological Society), 521.

Yang, T.-R., van Heteren, A., Wiemann, J., Chen, C.-J., and Spiering, B. (2016). Communal nesting behavior of dinosaurs revealed by statistical analyses of phosphorus distribution in, and external morphology of, eggshells. In A. Farke, A. MacKenzie and J. Miller-Camp (Eds.), *SVP 76th Annual Meeting*. Salt Lake City, UT: Society of Vertebrate Paleontology, 255.

Yang, T.-R., Wiemann, J., Xu, L., Cheng, Y.-N., Wu, X.-C., and Sander, P. M. (2019b). Reconstruction of oviraptorid clutches illuminates their unique nesting biology. *Acta Palaeontol. Polonica* 64. doi: 10.4202/app.00497.2018

Zelenitsky, D. K., and Therrien, F. (2008). Unique maniraptoran egg clutch from the Upper Cretaceous Two Medicine Formation of Montana reveals theropod nesting behaviour. *Palaeontology* 51, 1253–1259. doi: 10.1111/j.1475-4983.2008.00815.x

Zhao, Z.-K. (1975). The microstructure of the dinosaurian eggshells of Nanxiong Basin, Guangdong Province. 1. On the classification of dinosaur eggs. *Vertebrata PalAsiatic* 13, 105–117.

Zhao, B., Chen, Y., Lu, H.-L., Zeng, Z.-G., and Du, W.-G. (2015). Latitudinal differences in temperature effects on the embryonic development and hatchling phenotypes of the Asian yellow pond turtle, Mauremys mutica. *Biol. J. Linn. Soc.* 114, 35–43. doi: 10.1111/bij.12400